



Luminescence rock surface exposure and burial dating: a review of an innovative new method and its applications in archaeology

L. A. Gliganic¹ · J. McDonald² · M. C. Meyer³

Received: 18 May 2023 / Accepted: 30 November 2023

© The Author(s), under exclusive licence to Springer-Verlag GmbH Germany, part of Springer Nature 2023

Abstract

Luminescence rock surface burial and exposure dating approaches hold enormous potential to contribute to the archaeological sciences. These methods enable the dating of previously undatable archaeological site types and can be used to determine how and when lithic artefacts have been sequentially buried and transported. Studies have already used these approaches to overcome limitations of classical dating methods to constrain the ages of lithic artefact discard and post-depositional movement at surface scatter sites, to chronologically constrain rock art production by dating rockfall and exposure events, as well as dating a variety of rock-based archaeological features such as pavements, petroforms, megalithic structures, and walls. Here, we present a review of these developing methods, including an introduction to the underlying principles and applications, a series of case studies, and a discussion of the obstacles and complexities to be considered when applying these methods. We conclude with a discussion of future applications and developments, including direct dating of rock engravings, buried artefacts, megalithic stone structures, and chert artefacts. With ongoing work and applications, luminescence rock-surface dating has the potential to become widely applicable, shining new light on a diverse range of previously intractable archaeological contexts.

Keywords Luminescence · Rock surface dating · Exposure dating · Burial dating · Archaeology

Introduction

Archaeology is the study of material remains such as tools (stone, bone, wood, and metal), rock art (petroglyphs and pictographs), meals and implements (bones, residues on tools), and built structures (walls, cairns, postholes, megaliths, pavements) to understand past human behaviour. But studying these material remains in isolation says very little about past human behaviour unless those materials are understood within the context that they were created, used, and discarded: the site context, the environmental and climatic contexts, and social contexts. To succeed in understanding prehistoric human societies and in explaining past

human behaviour correctly, a secure temporal framework is required to appropriately scaffold a cohesive story about the past. Without the control of time, comparisons of archaeological assemblages may lead to erroneous interpretations (Harris 1979; Lucas 2012).

The rapid development and ongoing refinement of geochronological methods over the last 70 years has vastly improved our understanding of past human behaviour. Radiocarbon dating (Libby 1952; McDonald et al. 2014; Steelman and Rowe 2012; Steelman et al. 2021), uranium series dating (Hellstrom and Pickering 2015; van Calsteren and Thomas 2006), potassium-argon and argon-argon dating (McDougall and Harrison 1999; McDougall et al. 2005), and electron spin resonance dating (Rink 1997; Grün, 2006) are just some of the methods that have been applied to a huge range of archives, enabling a chronometric understanding of material culture at a range of sites. The use of luminescence as a geochronological tool began with the development of thermoluminescence (TL) dating, which allowed precise and secure dating of when quartz and feldspar minerals were heated, with applications for dating pottery (Fleming 1966; Zimmerman 1967) and heated lithic materials (Göksu et al. 1974; Richter and Krbetschek 2006;

✉ L. A. Gliganic
lukeg@uow.edu.au

¹ School of Earth, Atmospheric and Life Sciences, University of Wollongong, Wollongong NSW, Australia

² Centre for Rock Art Research and Management, University of Western Australia, Crawley WA, Australia

³ Institute for Geology, University of Innsbruck, Innsbruck, Austria

Richter 2007). The development of optically stimulated luminescence (OSL) dating of quartz and infrared stimulated luminescence (IRSL) dating of feldspar have allowed determination of when fine-grained quartz and feldspar-bearing sediments (i.e., silt to sand-sized sediments that make up a large fraction of the clastic sediment record) were last exposed to sunlight and buried (Huntley et al. 1985; Hütt et al. 1988). The direct dating of fine-grained sedimentary deposits via OSL and IRSL dating marked the second chronometric revolution in the earth and archaeological sciences (Jacobs and Roberts 2007; Roberts and Lian 2015; Murray et al. 2021) and both techniques are often also referred to as optical or luminescence dating.

The aforementioned chronometric techniques can be used to directly date anthropogenic use or interaction with some materials including wooden, shell, bone, and heated artefacts. However, human interaction with archaeological materials such as lithic artefacts and stone structures or intentional modification of rock surfaces, such as rock engravings, remain difficult to directly date. These kinds of lithic materials and anthropogenically modified rock surfaces can usually only be dated based on their physical association with different datable materials, such as their stratigraphic relationship to datable sediments or via cross-dating with known age artefacts or rock art based on typological criteria.

This is sub-optimal given the ubiquity of artefactual material at archaeological sites and the durability of stone as a raw material for tool construction in nearly all places and times in the past. Dating lithic artefacts based on their stratigraphic association with other datable materials has been a successful approach, particularly in buried stratified deposits like rockshelters and open excavations (Jacobs et al. 2008, 2011; Gliganic et al. 2012; Ames et al. 2020; McDonald et al. 2018; Slack et al. 2020; Wilkins et al. 2021). However, ascertaining chronological control for lithic artefacts with insecure or imprecise stratigraphic associations can be problematic and typological cross-dating approaches are fraught with uncertainties, preventing archaeologists from an accurate understanding of numerous archaeological sites and records. Sites where the stratigraphic association between the artefact and a datable substrate is weak or completely lacking are common in the archaeological record and include surface lithic artefact scatters, lithic raw material quarries, petroforms including stone arrangements and megaliths, and engraved rock art (petroglyphs).

Promising recent work has shown the potential of using optical luminescence signals (OSL and IRSL) from rock surfaces. This radically expands the scope of luminescence dating, from a chronometric approach applicable to only silt to sand-sized sediments to being applicable to a huge variety of geological and archaeological settings where coarse-grained (gravel to boulder) geological materials or archaeological features or rock surfaces are of interest. For example, OSL and IRSL rock surface dating have been

successfully used to constrain the timing of emplacement of gravel pavements and deposits in both archaeological (Sohbati et al. 2015; al Khasawneh et al. 2019a, b; Feathers et al. 2019, 2022; Ageby et al. 2021) and geological contexts (Simms et al. 2011; Jenkins et al. 2018; Bailiff et al. 2021; Cunningham et al. 2022). OSL rock surface dating has been used to disentangle the timing of brick emplacement in walls and buildings from the firing age of the bricks (Vieilleveigne et al. 2006; Galli et al. 2014, 2017). It has, likewise, been used to confirm the construction age of Egyptian and Greek tombs and monuments by dating the emplacement of rock slabs and blocks (Liritzis and Vafiadou 2015; Liritzis et al. 2019). OSL rock surface dating has also been used to constrain the exploitation of raw material quarries and associated lithic artefact discard (Gliganic et al. 2019, 2021) and the timing of a whetstone usage (Freiesleben et al. 2015). These variants of OSL rock surface dating use either (i) the degree of bleaching into a rock surface as a measure of sunlight exposure time (i.e. *rock surface exposure dating*; e.g. Freiesleben et al. 2015; Gliganic et al. 2019) or (ii) measurement of the re-accumulated luminescence signal from formerly bleached gravel or boulder surfaces to obtain rock burial ages. The latter approach is also known as *rock surface burial dating* and can be applied to, e.g. the light-shielded undersides of sub-aerially exposed rocks and lithic artefacts (e.g. Simms et al. 2011; Sohbati et al. 2015; al Khasawneh et al. 2019a; Feathers et al. 2019; Gliganic et al. 2021; Ageby et al. 2021) or to gravels that have been partly bleached and subsequently buried completely (Jenkins et al. 2018; al Khasawneh et al. 2019b; Bailiff et al. 2021; Cunningham et al. 2022).

These new luminescence rock surface dating approaches promise to enable the direct dating of human use and interaction with rock-based materials in the archaeological record. Here, we present a review of the methods, with an introduction to classical sedimentary luminescence burial dating (as it shares many methodological principles with rock surface burial dating), followed by a high-level description of the luminescence rock surface exposure dating and luminescence rock surface burial dating methods and their potential value to archaeological dating. Next, we present a series of case studies demonstrating the utility of such approaches in different archaeological contexts. This is followed by a review of caveats and issues when considering a luminescence rock surface dating campaign. We finish by discussing innovative approaches to improve the accuracy and precision of measurements and potential future applications.

Method

A general background of classical sedimentary optical dating

Optical dating has classically been used as a technique that can estimate the last time silt or sand-sized sediments

were exposed to sunlight and subsequently buried (Huntley et al. 1985; Aitken 1998). When a grain of quartz or K-feldspar is exposed to sunlight, the latent luminescence signal within the grain is erased, in a process called ‘bleaching’. When the grain is shielded from sunlight (e.g. during burial), exposure to cosmic rays and ionising radiation from the surrounding environment induces the accumulation of a latent luminescence signal (in the form of electrons trapped in defects in the crystal structure of the mineral grains). The longer a grain is buried, the longer the grain is exposed to ionising radiation, the larger the total amount of radiation the grain absorbs, and the larger the latent luminescence signal is that accumulates in the grain (Fig. 1a). The rate of latent luminescence signal accumulation is proportional to the flux of ionising radiation due to radioelements in the surrounding environment and cosmic rays (the ‘dose rate’). In the laboratory, quartz grains are stimulated with blue or green light and emit an optically stimulated luminescence (OSL) signal, while K-feldspar grains are stimulated with infrared (IR) light and emit an IR stimulated luminescence (IRSL) signal (Fig. 1b). The measured OSL or IRSL signal can be used to calculate the total radiation dose that the grain was exposed to during burial (the ‘equivalent dose’ or D_e). The burial age (ka) of a grain is calculated by dividing the D_e (Gy) by the dose rate (Gy/ka) (Fig. 1).

Samples for OSL or IRSL sediment burial dating are typically obtained by hammering stainless steel or plastic tubes into freshly cleaned outcrop faces and the sealed tubes are brought into the laboratory for further preparation under controlled red to orange light conditions. Sediment blocks can be obtained from compacted or cemented sediment layers and the light unexposed interior of these blocks can be used for sediment dating purposes. Pure extracts of quartz or K-feldspar are isolated from such bulk sediment samples using standardised procedures (Wintle

1997). Bulk sediment samples are soaked in hydrochloric acid (HCl) to remove carbonates and hydrogen peroxide to remove organic materials. The cleaned grains are then sieved for the desired grain size (often 180–212 μm). The target grain size is then density separated using heavy liquid (e.g. sodium polytungstate) to isolate the target minerals. Quartz grains (density of 2.62–2.70 g/cm^3) are separated from heavy minerals and feldspars using heavy liquid solutions. K-feldspar grains (density of 2.53–2.58 g/cm^3) are separated from sodium (Na)-feldspar and lighter minerals using heavy liquid solutions. The quartz and K-feldspar isolates are then etched with hydrofluoric acid to remove contaminant grains and remove the outer $\sim 9 \mu\text{m}$ of the grains. A final HCl soak and sieve are undertaken before extracts of the target minerals are prepared for measurement. Many grains can be mounted on stainless steel discs in a monolayer using an adhesive for multi-grain aliquot measurements. Alternatively, individual grains can be mounted onto aluminium single-grain discs (10 mm diameter with 100 300 μm -diameter holes) for measurement.

The luminescence signal measured from grains is usually converted to a D_e by undertaking single-aliquot regenerative dose (SAR) procedure measurements (Murray and Wintle 2000). This involves giving the grains repeated cycles of known radiation doses (regenerative doses) and measuring the luminescence response to those known doses. A small radiation dose (test dose) is applied and measured (T_x) following measurement of the natural (L_n) and regenerative dose (L_x) luminescence signals. The test dose signal is used to normalise the natural and regenerative dose signals to account for any changes in luminescence intensity per-unit-dose over the course of repeated cycles of dosing, heating, and optical stimulation. The test dose-normalised regenerative dose measurements (L_x/T_x) are then used to construct a dose–response curve, onto which the test dose-normalised

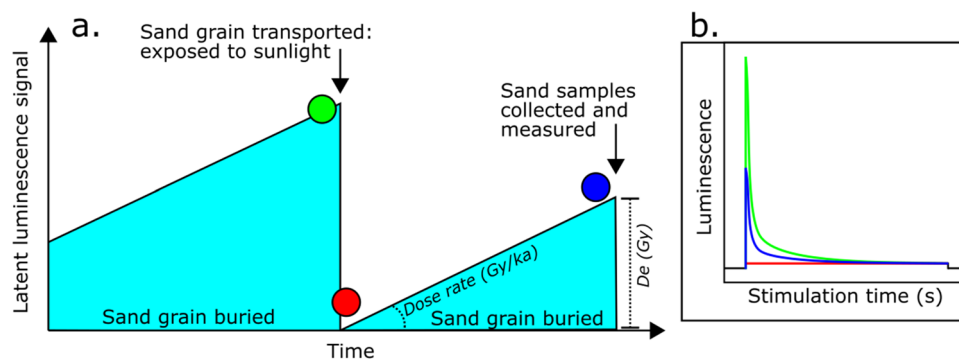


Fig. 1 Schematic showing the processes of luminescence signal bleaching and accumulation in sediments. **a** The relationship between the latent-luminescence signal in a sand grain and time during burial, transport and sunlight exposure, and a second burial phase; and **b** the

luminescence decay curves that would be measured at various points in **a**; the colour of the decay curves in **b** is related to the coloured circles in **a**

natural measurement (Ln/Tn) is projected to determine the De . For quartz grains, blue stimulation light is used, and an ultraviolet (UV) emission is measured. For K-feldspar grains, IR stimulation light is used, and a blue emission is measured. The quartz OSL signal is generally stable and can be used for accurate De measurement. The K-feldspar IRSL signal, however, suffers from anomalous fading, namely an athermal reduction in latent IRSL signal with time (Wintle 1973). Several methods can be used to overcome fading. First, the rate of fading can be measured and used to correct IRSL ages (Huntley and Lamothe 2001), though this requires extrapolating laboratory-measured fading rates over geological timescales. Alternatively, less- or non-fading signals can be accessed, such as the post IR-IRSL (pIRIR) and IR photoluminescence (IRPL) signals (Thomsen et al. 2008; Prasad et al. 2017).

The dose rate is derived from concentrations of uranium, thorium, and potassium in the sediments around the grains and from the grains themselves, as well as cosmic rays. The dose rate due to cosmic rays can easily be modelled and calculated based on the sample locations latitude, longitude, elevation, and sediment overburden (Prescott and Hutton 1994). The internal alpha dose rate of quartz grains is derived from trace amounts of U and Th and is very low—on the order of 0.03 ± 0.01 Gy/ka (Bowler et al. 2003). The internal dose rate of K-feldspar grains is higher than quartz due to the presence of ^{40}K and ^{87}Rb as well as U and Th in K-feldspar grains. It is frequently assumed (e.g. following Huntley and Baril 1997; Mejdahl 1987; and Huntley and Hancock 2001) but can also be measured (e.g. Smedley and Pearce 2016; O’Gorman et al. 2021). Typical K-feldspar grains of 180–212- μm diameter could include an effective internal beta and alpha dose rates of 0.80 ± 0.03 Gy/ka and 0.10 ± 0.03 Gy/ka, respectively (Gliganic et al. 2012). The

external dose rate derived from U, Th, and K in the surrounding sediments is delivered to the sampled grains in three forms: alpha particles, beta particles, and gamma rays (Aitken 1985). Alpha particles are attenuated within approximately 0.025 mm. The portions of grains that experienced alpha irradiation during burial are removed using a concentrated hydrofluoric acid (HF) etch, which removes the outer ~ 9 μm of each grain. Beta particles and gamma rays usually form the bulk of the total dose rate and can travel up to 3 mm and 30 cm, respectively, in sediments. Each source of ionising radiation, therefore, must be considered when sampling—if the sampled grains are within 3 mm or 30 cm of a medium with a different dose rate, then that must be taken into account. The external beta, gamma, and cosmic dose rates must then be corrected for the moisture content of the sample using correction factors (Aitken 1985) to account for absorption of radiation by interstitial pore water. The calculated burial ages increase by approximately 1% for each 1% increase in water content.

Luminescence rock surface dating

While classical luminescence dating uses silt and sand-sized mineral grains, it is also possible to measure the luminescence signals from the mineral grains that comprise rocks. Rock surface dating is based on the principle that in the interior of a sufficiently old sedimentary or crystalline rock the natural luminescence signal is always in saturation (Fig. 2a, d). Sunlight penetrates the rock surface as a function rock transparency, photon flux at the rock surface and time (see the following section), causing resetting of the natural luminescence signal stored in the mineral grains that constitute the outermost millimetre to centimetre of a given sample (Fig. 2b, e) (Sohbati et al. 2011, 2012a). Penetration

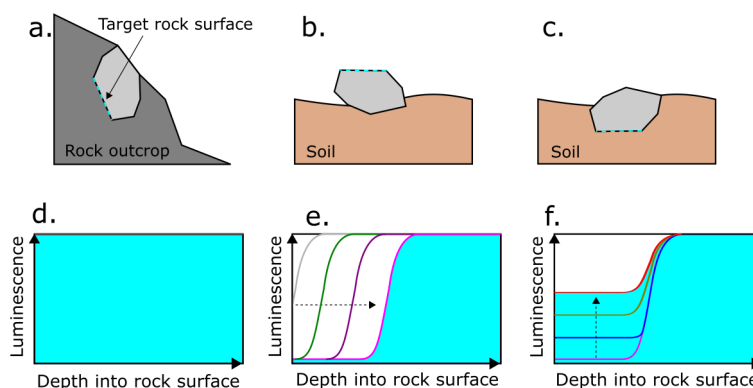


Fig. 2 Schematic representation of the processes underlying the luminescence rock surface dating approaches. **a–c** A stylised representation of the movements of a target rock surface in the environment through time from **a** being entombed in its geological rock context to

b being sub-aerially exposed following exhumation to **c** being partly buried. **d–f** How the latent luminescence signal at the rock’s surface changes with time in relation to the events in **a–c**

of light into solid rock is possible because most of the constituent minerals are not entirely opaque. This allows photons to penetrate into the rock's interior by exploiting light transparent rock textures such as interconnected grains of transparent minerals (e.g., quartz), thus forming 'light pipes' (Ou et al. 2018; Meyer et al. 2018). As a result, a bleaching front can be observed in most rock samples at several millimetre to centimetre depth below the surface (Fig. 2e). As detailed below, the depth and shape of this bleaching front (i.e. the portion of the luminescence-depth profile where the luminescence signal is between bleached and saturated) holds chronological information. It can be exploited to determine both sunlight exposure ages of exposed or previously exposed surfaces (via a rock surface exposure dating approach) and burial ages for currently or previously buried surfaces (via a rock surface burial dating approach) (e.g. Habermann et al. 2000; Liritzis 1994; Liritzis and Galloway 1999; Polikreti et al. 2003; Sohbaty et al. 2012a; Gliganic et al. 2021). A combination of these approaches is also feasible in unravelling the burial history of samples that experienced a complex combination of consecutive exposure and burial events (Freiesleben et al. 2015; Ageby et al. 2021).

Sample collection and preparation

Sampling for a rock surface dating approach (either burial or exposure) can sometimes be relatively simple, such as when small- to medium-sized samples (e.g., hand-sized surface artefacts, cobbles, or pebbles) are investigated. However, sampling natural rock walls, boulders, or large-scale anthropogenic blocks or monuments can require the use of dedicated drilling and cutting equipment. In the case of a rock surface burial approach, partial excavation of the sample base might be required to access the buried rock surface.

Rock samples must be collected in the dark and then kept in the dark throughout transportation. Samples should be prepared in the laboratory under controlled (red or orange) lighting conditions. Rock samples should be thick enough to encompass the bleached portion of the target rock surface and a representative section of the saturated (i.e. unbleached) portion of the rock (e.g. luminescence depth profile in Fig. 3c). The minimum rock sample thickness depends on the rock transparency, but is typically 2 to 5 cm. Sediment samples from below the rock surface should be collected for dose rate measurement.

Exposed rock surfaces collected for rock surface exposure dating would be collected by removing a portion of the rock surface, by either drilling a core from the surface or removing the rock surface with a rock saw. Smaller samples (gravels, cobbles, or surface artefacts) can be collected as bulk samples and stored in a light-safe way (e.g. wrapped in aluminium foil), particularly if aiming for a combined rock

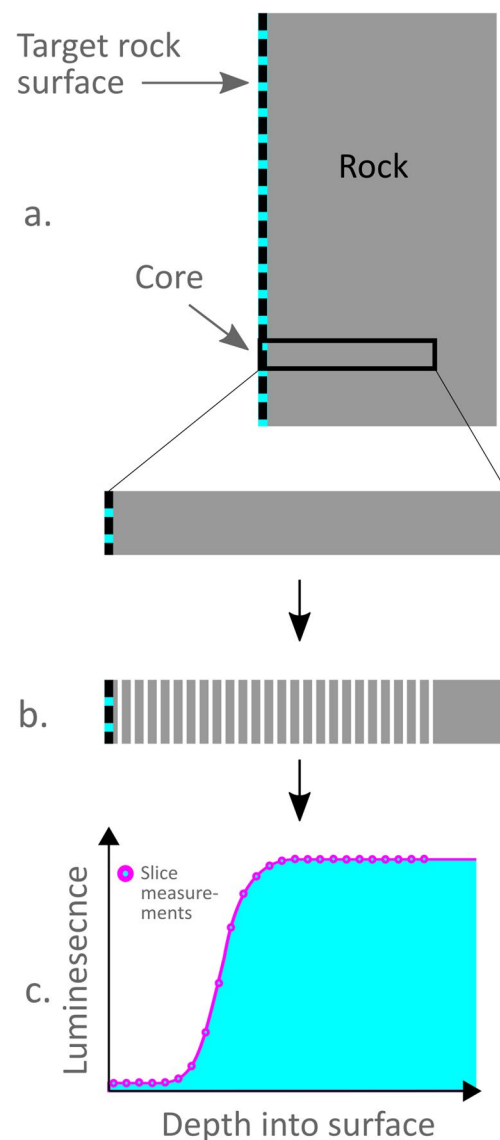


Fig. 3 Schematic showing typical sample preparation steps. **a** A core is collected from the target rock surface (dashed blue-black line). **b** The core is sliced in ~1-mm increments. **c** The luminescence signal is measured for each slice and is plotted as a luminescence-depth profile: Luminescence is plotted on the y-axis and the depth of the slice into the rock surface is plotted on the x-axis

surface exposure and burial dating approach (e.g. Bailiff et al. 2021). Furthermore, for rock surface exposure dating, the following information should be collected during sample collection for an accurate age calculation and evaluation (see the following section): (i) inclination and aspect of the sampled rock surface, (ii) eventual light shielding of the sampled rock surface (e.g. shadowing effects), and (iii) a calibration sample of known age.

The next steps are conducted under red light conditions in the laboratory and are aimed at determining the luminescence-depth profile for a given rock sample using

the luminescence signal from a set of sub-samples usually obtained from a core. For both burial and exposure dating, it is important to know both the precise location within the rock surface of the sub-samples that are measured and to obtain these sub-samples at a spatial resolution as high as possible (typically in mm to sub-mm increments), so as to resolve the shape and depth of the bleaching front as precisely as possible. The following procedures depend on the type of rock. Very friable lithologies, such as some sandstones, can be surface abraded in precise increments (e.g. 1 mm) and the grains collected (Chapot et al. 2012). These grains can then be sieved for the desired grain size, mounted on stainless steel discs, and measured in the TL/OSL reader. For harder rock types, cores (~8.5–10-mm diameter) are drilled perpendicularly into the target surface using a water-cooled diamond core drill mounted on a drill press (Fig. 3a). These cores are then sliced in small increments (e.g. 1 mm) using a thin (~0.3 mm) diamond wafering blade on a water-cooled low speed saw—this yields a series of slices whose depths-below-the-rock-surface are precisely known (Sohbati et al. 2011) (Fig. 3b). These slices are then crushed to grains, which would be sieved before mounting onto stainless steel discs and measured in the TL/OSL reader. Alternatively, these slices can be placed in cups for direct TL/OSL measurement. To obtain precise luminescence measurements in the latter case, it is important to ensure proper thermal coupling between the rock slices and the heater plate of the TL/OSL reader. Towards that end, it has been suggested to pay particular attention to the thermal measurement parameters (heating rate and duration of isothermal hold) and to use metal cups to maximise thermal conductivity (Jenkins et al. 2018; Elkadi et al. 2021).

Luminescence rock surface exposure dating principles

Luminescence rock surface exposure dating reveals fundamentally different information to classical luminescence burial dating. It is used to estimate how long a rock surface has been exposed to sunlight. Luminescence rock surface exposure dating can yield similar information to cosmogenic nuclide exposure dating, though on different spatial and temporal scales, as we shall see.

Inside a host rock at a certain distance away from any natural or artificial rock surface (typically on the order of a few centimetres), the grains that comprise that rock will almost always have been shielded from heat and light for long enough to have saturated latent luminescence signals (target rock surface—see blue dashed line in Fig. 2a, d). Similar to the build-up of luminescence in fine-grained sediments, naturally occurring ionising radiation also causes the build-up and ultimate saturation of the latent luminescence

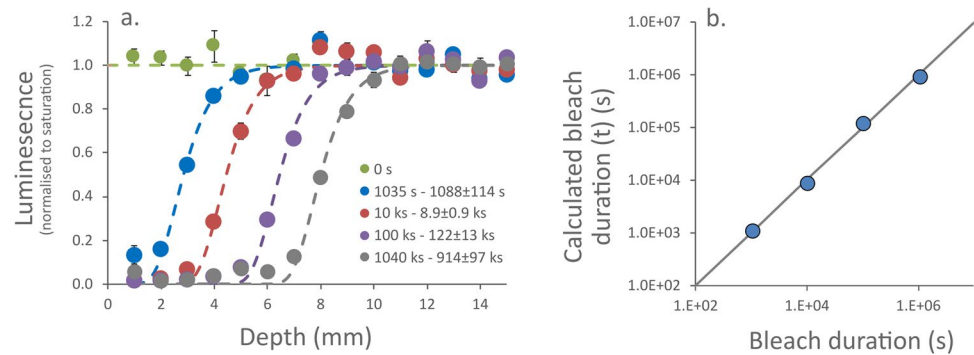
signal in a rock sample; however, in the case of a host rock, it is mainly due to the dose rate from the rock's interior. When the rock reaches the Earth's surface and becomes subaerially exposed, grains at the newly exposed rock surface are exposed to sunlight and their latent luminescence signal is bleached (Fig. 2b, e). As the rock surface is continuously exposed to sunlight for longer durations, the bleaching of latent luminescence will penetrate deeper into the surface—the longer the exposure duration, the deeper the bleaching depth (Fig. 2e). Bleaching will continue to penetrate into the rock's interior, until a steady-state between the surface bleaching rate and the dose rate of the host rock is achieved, defining the upper dating limit of this technique (Sohbati et al. 2012a; b).

Sohbati et al. (2011, 2012a) proposed that the dependence of the luminescence signal on depth-into-rock-surface and exposure-time could be described by a double exponential function:

$$L = L_0 e^{-\overline{\sigma\varphi_0}t} e^{-\mu x} \quad (1)$$

where L is the luminescence signal measured at depth x (mm) after exposure time t (s) and L_0 is the luminescence signal in saturation. $\overline{\sigma\varphi_0}$ (s^{-1}) is the effective de-trapping-rate constant describing an integral of the product of the wavelength-dependent photo-ionisation cross-section (σ ; cm^2) and photon flux at the rock surface (φ_0 ; $cm^{-2} s^{-1}$). The attenuation coefficient, μ (mm^{-1}), characterises light penetration into the rock. This model assumes (i) first-order kinetics for luminescence decay (an assumption that is applicable to quartz OSL but not to feldspar IRSL dating; Rasheedy 1993; Freiesleben et al. 2022), (ii) that the light spectrum does not change with depth-into-rock, and (iii) that the light intensity attenuates exponentially with depth-into-rock. The model predicts that the longer the exposure duration, the deeper the resetting of the luminescence signal into the rock surface, which has been demonstrated in controlled laboratory settings (Fig. 4a). Gliganic et al. (2019) performed a laboratory-controlled experiment in which they used $\sim 3 \times 3 \times 3$ cm cubes of quartzite material with saturated latent OSL signals. All cubes were placed in a solar simulator (Hönle Sol 500) at the same time and were then removed, one by one, after 1035 s, 10 ks, 50 ks, 100 ks, and 1040 ks. One additional cube was not placed in the solar simulator (0 s) and served as a control. The results of this experiment showed that longer laboratory bleaching durations yielded deeper OSL-depth profiles, thereby validating the fundamentals of luminescence rock surface exposure dating approach as a relative dating tool for rock surfaces with different exposure ages (Fig. 4a). Sohbati et al. (2012b) further developed the luminescence surface exposure dating model by including the simultaneous effect of daylight bleaching and environmental dose rate. This

Fig. 4 The laboratory-controlled bleaching experiment of Gliganic et al. (2019) showing **a** OSL-depth profile data and best-fit models for five identical blocks bleached for five different durations in a solar simulator; **b** plot of the measured exposure duration (t) (s) against the known exposure duration (s) with the 1:1 line also shown



extended bleaching-with-depth-model bears relevance for rock surface dating applications of very old rock surfaces (> 10–100 ka), where the competing effects of both optical resetting due to daylight bleaching and simultaneous natural irradiation due to the rock's internal dose rate need to be considered (Sohbati et al. 2012b), as do the effects of rock surface erosion (Sohbati et al. 2018).

While there exists chronological information in luminescence-depth profiles from an exposed rock surface, some of the parameters, namely $\overline{\sigma\varphi_0}$ and μ parameters, must be constrained to determine the absolute exposure time. Unfortunately, it can be challenging to quantify the model parameters from the first principles (Sohbati et al. 2011). One solution is to quantify the $\overline{\sigma\varphi_0}$ and μ parameters using a known-age calibration surface of the same lithology as the unknown age surface (Sohbati et al. 2012a; Gliganic et al. 2019). In this case, luminescence-depth profiles are measured from known age surfaces. The luminescence-depth profiles are fitted with Eq. 1, holding t constrained and fitting for $\overline{\sigma\varphi_0}$ and μ . The optimised $\overline{\sigma\varphi_0}$ and μ parameters are then constrained when fitting the unknown-age target rock surface sample. Known-age calibration surfaces can range from historical (i.e. a road cutting of known age—Sohbati et al. 2012a) to surfaces created when sampling the target sample (i.e. treating the scar produced by collecting the target surface as the calibration surface—Gliganic et al. 2019). Given the sensitivity of the modelled bleaching to orientation, sunlight aspect, and local bleaching conditions, it is important that the calibration surface be exposed in yearly increments (to avoid seasonal differences in insolation) and have the same orientation and aspect as the target surface (Fuhrman et al. 2022). In the laboratory bleaching experiment of Gliganic et al. (2019), Eq. 1 was fitted to the OSL-depth profiles of all the known-age, laboratory-bleached blocks (excluding one outlier). The results indicated that accurate estimates of known exposure durations could be achieved using other known-age surfaces, thus confirming the method's usefulness as an absolute dating tool (Fig. 4b).

Luminescence rock surface burial dating principles

Luminescence rock surface burial dating is predicated upon the same principles as sedimentary luminescence burial dating and yields the same kind of chronological information, namely the burial duration of a rock surface. When a rock surface is exposed to sunlight, the luminescence signal in the mineral grains that comprise that surface is bleached (Fig. 2b, e). When the rock surface is subsequently shielded from sunlight, such as during burial or being flipped so as to be in contact with the ground surface, a latent luminescence signal begins to accumulate in the mineral grains at a rate proportional to the flux of cosmic rays and concentrations of U, Th, and K in the surrounding sediment and the rock itself (Fig. 2c, f).

Two approaches can be used to calculate burial ages for rock surfaces, both of which can often be applied to a given sample as a form of pseudo-independent age corroboration. The first is a classical approach in which the total dose absorbed by the grains comprising the rock surface (De) is divided by the total experienced dose rate to calculate the burial age. In this case, De values are relatively straightforward to estimate—they can be measured for each slice using the SAR procedure. The measured De values can then be plotted as a function of depth within the rock surface to create a De -depth profile for the target surface (i.e. spatially resolved De values). The appropriate dose rate for each slice is more complicated to estimate. Implicit in rock surface burial dating is that the target sub-samples, namely the rock slices that are to be measured, will have beta and gamma dose rate contributions from different media (i.e., the rock itself and the sediment adjacent to the rock) which will likely have different radionuclide concentrations. Beta particles travel approximately 3 mm in sediments and rock while gamma rays travel up to 30 cm. Hence, the irradiation sphere of a beta and gamma emitting radionuclides are ~ 3 mm and ~ 30 cm in radius, respectively. These differences and their spatial distribution need to be explicitly considered for dose rate calculations in rock surface burial

dating. For example, the surface slice of the rock will have approximately 50% of its beta contribution from the sediment and 50% from the rock, but the mineralogical composition and thus radionuclide concentration in the rock and in the underlying sediment will likely differ from each other. Hence, the dose rates of the underlying sediment and of the rock must be determined separately. Due to their long range, the proportions of gamma ray irradiation will also depend on the geometry of the rock and its relative position within the sediment profile. A spatially resolved depth-into-rock-surface dose rate model must thus be created using the sediment- and rock-specific dose rates and the geometry of the rock sample in its site context (e.g. following Aitken 1985; Sohbati et al. 2015; Gliganic et al. 2021). The spatially resolved and geometry-corrected dose rates can then be used with the spatially resolved De values to calculate spatially resolved ages into the target rock surface (an age-depth profile). Plateaus in the age-depth profiles can then be used to (i)

identify burial ages, (ii) discern multiple phases of exposure and reburial, and (iii) investigate whether the rock surface was well bleached prior to burial (Gliganic et al. 2021; al Khasawneh et al. 2019a,b; Rades et al. 2018; Sohbati et al. 2015; Jenkins et al. 2018).

The second approach involves fitting the luminescence-depth profile into a rock surface with Eq. 4 of Freiesleben et al. (2015), shown here as ‘First burial (B1)’ in Table 1. A powerful application of luminescence rock surface dating combines Sohbati et al.’s (2012a) Eq. 1 (see Eq. 1) and Freiesleben et al.’s (2015) Eqs. 4 and 8 to identify multiple exposure and burial events within a single rock surface and calculate their ages. This modelling approach has been developed by Freiesleben et al. (2015) and is conceptualised graphically in Fig. 5 a. The individual fitting steps involved in modelling sequential exposure and burial events and their respective analytical expressions are given in Table 1 and are based on first-order kinetics. The model assumes that the final condition (the result of one event) becomes the initial condition for the subsequent event. The first exposure event (E1) creates the blue bleaching profile in Fig. 5a that can be fitted with equation L1 from Table 1. This curve, in turn, becomes the initial condition for the subsequent burial event (B1; black profile line in Fig. 5a) that can be fitted with equation L2. The model fitting parameters in Table 1 are the luminescence intensity at depth x ($L(x)$), the saturated luminescence intensity (L_0), the light attenuation coefficient (μ), the effective detrapping-rate constant $\overline{\sigma\varphi_0}$ (s^{-1}), and the rate of electron trapping/luminescence accumulation: $F(x) = \frac{\dot{D}}{D_c}$ where \dot{D} is the effective dose rate at depth x and D_c is a sample-dependent averaged constant characterising the filling rate of the electron traps. The model also includes the exposure time (t_e) and the subsequent burial time (t_b).

Table 1 Model developed by Freiesleben et al. (2015) to fit for multiple burial and daylight exposure events. The model profiles are normalised to 1 (luminescence saturation)

Event	Fitting model
Initial burial	$L_0(x) = 1$
First exposure (E1)	$L_1(x) = L_0(x)e^{-t_{e1}\overline{\sigma\varphi_0}e^{-\mu x}}$
First burial (B1)	$L_2(x) = (L_1(x) - 1)e^{-F(x)t_{b1}} + 1$
Second exposure (E2)	$L_3(x) = L_2(x)e^{-t_{e2}\overline{\sigma\varphi_0}e^{-\mu x}}$
Second burial (B2)	$L_4(x) = (L_3(x) - 1)e^{-F(x)t_{b2}} + 1$
Etc	...

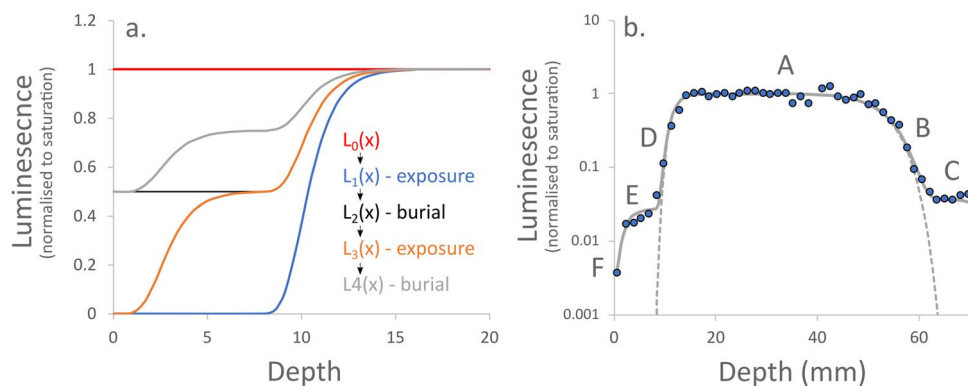


Fig. 5 **a** Modelled luminescence-depth profiles (normalised to saturation) following Freiesleben et al. (2015) showing multiple sequential burial and exposure events. In this example, the sequence of events is a long period of burial sufficient to saturate all luminescence traps (L_0), followed by exposure (L_1), burial (L_2), exposure (L_3), and burial (L_4). **b** Measured luminescence (IR50)-depth profile from a granite

cobble showing multiple exposure and burial events (events A–F) at both the top and bottom surfaces. Data points reflect slice Ln/Tn data, the solid black line shows the Freiesleben et al. (2015) model fitted to the Ln/Tn data, and the grey line shows the modelled profiles prior to the last burial events. Figure modified from Freiesleben et al. (2015)

Case studies

Here we discuss several case studies in which the previously described luminescence rock surface dating approaches were used to temporally constrain a range of difficult-to-date archaeological sites. Some key takeaways are presented, as well as a more detailed description of the technical aspects and approaches of the studies.

Dating the Barrier Canyon Style rock art, Utah (Chapot et al. 2012; Sohbati et al. 2012a; Pederson et al. 2014)

Key takeaways

- The aim was to establish when this Great Gallery type-panel of Barrier Canyon Style rock art was made. While there are currently no absolute ages for this rock art style, it has been modelled to date to the last 1500–4000 years, predating the introduction of the bow and arrow and the Fremont culture (Schaafsma 1990).
- Ages for landscape geomorphic formation included fluvial terraces below and the formation of the alcove where paintings are located, with stratigraphic relationships used to determine the maximum possible age for when paintings could have been made and to hypothesise when paintings could have most easily been made.
- A combination of OSL rock surface burial dating and OSL rock surface exposure dating was used on a talus block containing part of an iconic painted motif that had suffered breakage through a rockfall event. The rock surface burial age reveals the minimum age for rock art (i.e. when the painted talus block detached from the alcove, confirmed by AMS dating of a trapped leaf) while the rock surface exposure age tells how long the block was exposed in the alcove before rockfall, indicating the window of possibility for when the paintings were made.

Description

Rock art is one type of material culture that remains extremely difficult to date. The Barrier Canyon Style (BCS) is a distinct rock art style of debated age found across the Colorado Plateau, USA. The authors investigated the type site for the BCS and used two approaches to determine a maximum possible age and minimum possible age for a motif there. The maximum age was determined based on the geomorphic relationships between landscape features and ages of the site context and the panel on which the rock art is situated. The art is located within a confined canyon with a series of terraces. The panel on which the rock art is situated could only have been exposed after incision of the upper

terrace, and the ~8000-year-old depositional age for the top of T2 deposits serves as a maximum possible age for the rock art. Given the geomorphic processes operating in the canyon, the authors suggest ~6000 years is a more plausible maximum age bracket for the exposure of the alcove. The more recent terrace formations provide further circumstantial evidence for the timing of painting—the basal T1 deposits date to ~3000 years and T1 was deposited in three distinct packages of flood deposits, dating to ~3000, 2300–1200, and 1100–800 years old. The height of the paintings relative to preserved T1 deposits on the opposite side of the canyon suggests that the paintings were made during the aggradation phase of T1 prior to erosion that has lowered the channel to its current level, leaving the paintings high above the surface (Pederson et al. 2014).

Determining the minimum age was possible because one of the iconic painted figures in the gallery has been affected by rockfall that removed its bottom half. The talus block on which the bottom of the figure was painted could be dated to date the age of the rockfall and how long the rock had been exposed prior to the rockfall event. This rockfall event was dated using three approaches. Rock surface burial dating of the down-facing (buried) surface of the talus block on which the art was painted yielded an age for when that surface was shielded from sunlight (i.e. when the block fell off). An OSL-depth profile taken from an exposed surface on a nearby rockfall talus block demonstrated that these rocks were well bleached by sunlight at the study site. Sedimentary OSL burial ages for sediment underlying the talus block yielded an age for when those formerly surface sediment were shielded from light (i.e. when the block fell off and covered the sediments). And a leaf that was serendipitously trapped between the underlying sediment and the talus block was AMS radiocarbon dated demonstrating when the leaf died and was trapped between the boulder and sediment. All three samples yield ages of between 800 and 900 years ago, yielding a solid minimum age constraint for the rockfall event, which happened after the painting was made (Chapot et al. 2012; Pederson et al. 2014).

They also measured an OSL-depth profile into the buried surface of the talus block (i.e. the surface that had formerly been exposed on the wall and on which the art was painted). They used this OSL-depth profile, with an OSL-depth profile from a known-age surface of the same lithology with similar aspect and shading conditions (namely an 80-year-old road cutting) and the currently exposed talus block, to calculate a pre-burial exposure age of ~700 years for the surface with the rock art (Fig. 6). They measured OSL-depth profiles into all samples, used the known-age sample to calibrate $\overline{\sigma\phi_0}$, and used a global fit of the calibration sample, the target sample, and the currently exposed sample to calibrate μ . With $\overline{\sigma\phi_0}$ and μ constrained, exposure durations of both the target surface

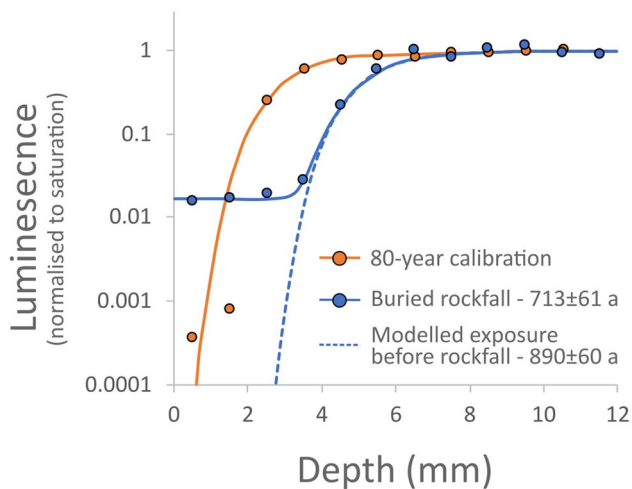


Fig. 6 OSL-depth profiles into buried surface of rockfall (blue) and 80-year-old calibration sample (red)—data points are slice OSL data, solid lines show Eq. 1 fit to data, and dashed line shows Eq. 1 fitted as if burial of rockfall surface did not occur. The panel surface had been exposed for 713 years before the rockfall event that buried it for the subsequent ~900 years. Modified from Pederson et al. (2014)

and the currently exposed surface were determined. Given the geomorphic context (namely the preponderous of talus in the T2 stratigraphy and the sequence of exposed sheeting joints in the sandstone wall indicative of recurring rockfall events), the authors interpret the rock surface exposure and burial chronology for the fallen block as indicating a penultimate rockfall event ~1600 years ago that exposed the panel on which the BCS figures were painted, before a subsequent rockfall event at ~1100 years that removed part of the panel and rock art. The most likely window for the painting of the Great Gallery BCS rock art figures was therefore concluded to be between ~1600 and ~1100 years ago. This fits at the later end of the projected age range for the Barrier Canyon style (Schaafsma 1990). The authors propose (Pederson et al. 2014: 12,990) that multiple rock art traditions operated in the greater Fremont temporal window, and that the BCS may have co-existed with the origins of the Fremont culture (and the introduction of bow and arrow), documented in this same time frame.

Tibetan raw material quarry and artefacts (Gliganic et al. 2019, 2021; Meyer et al. 2020)

Key takeaways

- Rock surface burial dating approach can be used to date sub-aerially exposed lithic flakes, including the detection of multiple phases of burial and exposure in artefacts.
- Rock surface exposure dating principles were validated in controlled laboratory experiments and an exposure age

was determined for a flake scar from a lithic quarry in Tibet

- OSL-depth profiles from surfaces of identical exposure age and lithology show significant differences in shape due to differences in mineralogy and possibly aspect

Description

Su-re is a quartzite lithic quarry and open artefact scatter site in south-central Tibet. The authors used a multi-disciplinary approach to investigate the site, including reconstruction of the complex local palaeoenvironment using geomorphological observations, sedimentary OSL burial dating and radiocarbon dating of landforms, OSL rock surface burial dating of discarded artefacts, and OSL surface exposure dating of a flake scar on a quarried boulder. The geomorphology set boundaries on the maximum ages for discarded artefacts and provided possible processes to explain some of the data.

Six quartzite artefacts that had been embedded in the ground surface that lay stratigraphically on a mid-Holocene pedo-complex were collected for luminescence rock surface burial dating. The buried surfaces of the artefacts were cored, sliced (1 mm increments), and crushed to grains, which were measured as multi-grain aliquots. A post-IR blue OSL signal was bright, shown to be appropriate for accurately measuring known radiation doses in the laboratory, and was used to measure D_e values for each aliquot. Spatially relevant dose rates were calculated for each slice and the resulting OSL age-depth profiles were produced. Plateaus in the age-depth profiles reflected a multi-step process including a long period of exposure (sufficient to bleach the pre-existing OSL signal deeply into the artefact) followed by burial of the surface and subsequent signal accumulation. Interestingly, multiple plateaus could be observed in one artefact, indicating a complex depositional history including at least two phases of exposure and burial (Fig. 7a). The artefact chronology from some artefacts indicated discard ~5.2 ka on top of (and concurrent with) a phase of mid-Holocene soil formation and associated optimal environmental conditions. Other populations of ages include ~2.4 ka and ~0.5 ka, coincident with late-Holocene and Little Ice Age phases of landscape instability, erosion, and redeposition identified in the geomorphological record. Combined, the chronology suggests site use and artefact discard during the mid-Holocene, followed by subsequent pulses of landscape instability that re-mobilised some artefacts. These findings clearly demonstrate that surface artefacts can record complex exposure and burial histories and that transport pathways of lithic clasts through the landscape can be revealed by a luminescence rock surface dating approach.

Additional work at Su-re included luminescence rock surface exposure dating work on the quarried boulders. Gliganic

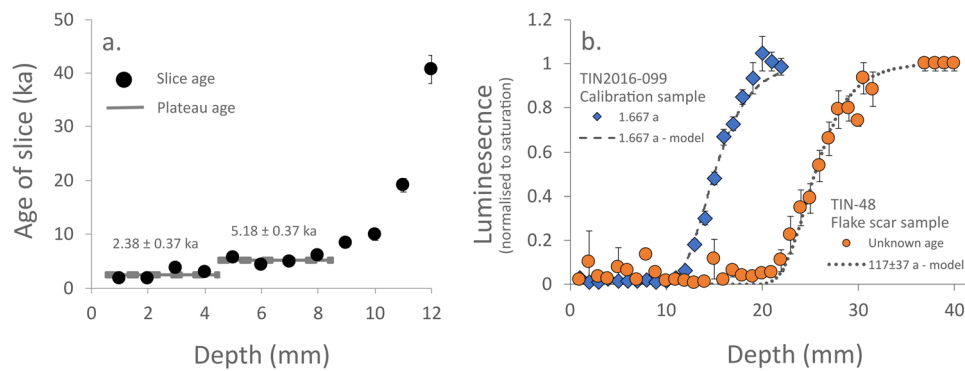


Fig. 7 **a** Age-depth profile calculated using the De values calculated for each slice and the spatially resolved dose rate into the underside of a quartzite surface artefact from Tibet. Age plateaus are shown as solid lines (error shown as dashed lines). Note that this profile shows two sequential burial events (at 5.18 ± 0.37 and 2.38 ± 0.37 ka) separated by a brief exposure event of unknown duration. Modified from Gliganic et al. (2021, Fig. 5). **b** OSL-depth profiles fit with Eq. 1 for

a known-age calibration sample (TIN2016-099; blue; 1.66 a) and an unknown age sample (TIN-48; orange). Data points are Ln/Tn values from slices. The calibration sample was fitted with Eq. 1 to derive $\sigma\phi_0$ and μ parameters, which were used to fit Eq. 1 to the TIN-48 data and derive an exposure age. Modified from Gliganic et al. (2019, Fig. 4)

et al. (2019) performed a controlled laboratory experiment whereby a suite of identical rock samples with saturated OSL signals were exposed to varying durations of solar simulator light ranging from 0 s (control) to 1040 ks (~12 days). OSL-depth profiles showed that increased light exposure duration yielded more deeply bleached OSL signals, thereby confirming the principles of the method for the first time under controlled conditions. Additionally, Eq. 1 could be fitted to the OSL-depth profiles (excluding one outlier) to accurately estimate the known exposure durations of the blocks, confirming the method's promise as an absolute dating tool (Fig. 4).

An exposure age was determined for an unknown-age flake scar. The known-age scar remaining after having previously collected the target unknown-age flake scar was used as a calibration surface. In this way, the calibration surface had a precisely known exposure age (1.667 a) and identical lithology and irradiation aspect to that of their target surface. The calibration sample yielded a measurable OSL-depth profile that could be used to calibrate the model and estimate that the flake scar had been exposed for ~117 years (Fig. 7b).

Dating a Danish whetstone (Freiesleben et al. 2015)

Key takeaways

- Freiesleben et al. (2015) described a new mathematical model to quantify both burial and exposure events based on luminescence-depth profiles from a given rock.
- They tested the model on a granite cobble used as a whetstone from a 2000-year-old archaeological site in Denmark.
- Luminescence-depth profiles and modelling show that the cobble was well bleached before burial and a history

of bleaching and deposition could be established that agrees with independent age controls: the bottom surface of the cobble yielded a burial age of 1.73 ± 0.16 ka. The upper surface of the cobble yielded more information, showing that it was collected for use by people 1.8 ± 0.5 ka, followed by 0.5 ± 0.4 ka of use (exposure), 1.3 ± 0.2 ka of burial in the site (burial), and 7 months of exposure after excavation.

Description

The main aim of the Freiesleben et al. (2015) study was to develop and describe a new mathematical model built on Eq. 1 to quantify repeated sequential events of exposure to daylight and burial in luminescence-depth profiles. To test the model, a granite cobble unearthed during a rescue excavation of an archaeological site dated to 2.00 ± 0.10 ka near Aarhus, Denmark, was used. The cobble had been part of the floor of a building and had been used as a whetstone in the past. Following excavation, it was discarded with the bottom, unworked side facing down and the upper side exposed to sunlight for 7 months before collection and measurement.

In the laboratory, cores were drilled through the entire cobble so that measurements could be made of both upper and lower surfaces. Cores were cut in 1.5-mm increments and the whole slices were measured directly using a high-temperature pIRIR290 SAR protocol. Their chosen stimulation and measurement protocol yielded sub-optimal dose recovery results (0.81 ± 0.02 and 0.85 ± 0.01 for IR50 and pIRIR290 signals, respectively) but low fading rates for appropriate given dose sizes (0.66 ± 0.20 and $0.24 \pm 0.10\%$ /decade for the IR50 and pIRIR290 signals, respectively), so no fading corrections were made.

The pIRIR290 signal was not fully bleached in the cobble. Luminescence-depth profiles for the IR50 signal show that both surfaces of the cobble were well bleached by significant daylight exposure prior to burial and multiple phases of burial and exposure could be identified. This can be seen in the IR50 profile (Fig. 5b), which shows one exposure event followed by a burial event in the bottom surface (events B and C), while the top surface shows a first exposure event followed by a burial event followed by a second exposure event (events D, E, and F). Event A represents the saturation level within the cobble.

The burial event observed in the bottom surface was dated by taking the average of the calculated ages for the first five surface slices, which were statistically consistent. This indicated that the bottom of the cobble was shielded from sunlight 1.73 ± 0.16 ka (event C). The upper surface of the cobble was complicated by the 7 months of post-excavation sunlight exposure (event F). Here, the IR50-depth profile of the upper surface was fitted with the new model and derive a burial age of 1.3 ± 0.2 ka (event E) using the D_c value from the bottom surface to fit for t_{b1}/D_c from the upper surface. They used the known age of event F to calculate the $\overline{\sigma\phi_0}$ parameter and calculate the exposure age for the older exposure event (event D), yielding an exposure duration of 0.5 ± 0.4 ka. In sum, the upper surface was exposed for 0.5 ± 0.4 ka (event D) before being buried for 1.3 ± 0.2 ka (event E), followed by excavation and exposure for 7 months (event F), indicating that the cobble was first used by people $\sim 1.8 \pm 0.5$ ka. This age is consistent with the burial age from the bottom of the cobble and from independent age controls.

Dating a Rodedian pavement in Israel (Sohbati et al. 2015)

Key takeaways

- A multi-method approach yielded internally consistent ages for when a cobble was emplaced into a pavement at a Rodedian site. The fading-corrected IR50 and pIRIR225 ages from the cobble surface and the quartz OSL age and the K-feldspar fading-corrected IR50 age from the sediment under the cobble are all consistent, but significantly underestimate the expected age.
- Luminescence-depth profiles from cobble indicate that it was well bleached when it was emplaced in its current position and that it had experienced multiple exposure and burial events. This indicates that (i) the cobble ages and consistent sedimentary ages were not affected by incomplete bleaching, and (ii) that the younger-than-expected ages for cobble emplacement might represent later intervention at the site and presumably movement of the cobble.

- Important information about the bleaching and depositional histories that was not available in unconsolidated sediments could be observed in the luminescence-depth profiles from rock surfaces. The cobble surface was explicitly shown to have been well bleached when emplaced, and earlier phases of exposure and burial could be observed.

Description

The Rodedian study site consisted of a scattering of suspected Late Neolithic flakes and a series of stone features, including a pavement, on a quartz-porphry dike ridge in the Negev Desert in Israel. One small paving cobble (15 cm × 10 cm × 8 cm) and the sediment accumulated underneath were collected for luminescence rock surface burial dating and sedimentary burial dating.

Quartz and K-feldspar separates from the sediments were isolated using standard techniques. A grain size of 63–90 μm was probably dominated by aeolian material and presumed most likely to have been sufficiently bleached before deposition. The OSL signal from sixteen 8-mm multigrain aliquots of quartz yielded an age of 4.2 ± 0.4 ka. A pIRIR225 protocol was used to measure K-feldspar grains (Buylaert et al. 2009). Fading rates were measured following Auclair et al. (2003) and g -values calculated following Huntley and Lamothe (2001) were used to calculate fading-corrected IR50 and pIRIR225 ages. Thirty-three 2-mm multi-grain aliquots yielded fading-corrected IR50 and pIRIR ages of 4.3 ± 0.3 ka and 5.9 ± 0.4 ka, respectively. While the IR50 age agrees with the quartz age, the pIRIR225 age is apparently older. This is not surprising since the pIRIR225 signal bleaches more slowly than either the quartz OSL and K-feldspar IR50 signals, suggesting that it may have only been partially bleached.

The cobble samples were prepared using standard methods. Cores (> 20 mm long) collected from the buried surface of the cobble were cut into slices of ~ 1.5 -mm thickness. The surface slices were soaked in HF (10% for 40 min) and HCl (10% for 20 min) to remove surface weathering products while the inner slices were not treated with acid. Whole slices were measured following the same measurement protocol used for K-rich feldspar sediment grains, yielding fading-corrected IR50 and pIRIR225 ages (n = eight surface slices) of 4.3 ± 0.3 ka and 4.1 ± 0.2 , respectively. Since the IR50 and pIRIR225 signals have significantly different bleaching rates, the consistency in ages derived from both signals in the cobble strongly indicate that it was well bleached before being emplaced. These ages are indistinguishable from the quartz OSL and K-feldspar IR50 ages from the underlying sediments, adding strength to the case that the luminescence signals from these signals were well bleached at deposition.

To explicitly check whether the luminescence signal at the surface of the cobble was fully bleached before it was incorporated into the pavement, luminescence-depth profiles (L_n/T_n vs depth) were measured for three cores into the buried surface of the cobble. The IR50 signal (Fig. 8a) is bleached more deeply than the pIRIR225 signal (Fig. 8b), corroborating that the pIRIR225 signal is harder to bleach. The luminescence-depth profiles show a gentle rise, followed by flattening and subsequently a steep rise towards signal saturation. When the profiles are modelled following Freiesleben et al. (2015), the predicted profiles show that the IR50 and pIRIR225 signals were reset to depths of ~ 7 and ~ 2 mm, respectively, before emplacement in their current position, thereby validating that the resulting ages are not impacted by incomplete bleaching. The predicted profiles also show evidence for an older bleaching and burial event, though no age could be derived for that event (Fig. 8).

The luminescence-depth profiles explicitly demonstrated that the cobbles were well bleached before deposition in their current state. The consistency in the cobble ages and the sedimentary quartz OSL and K-feldspar IR50 ages strongly supports this suite of ages, centred on 4.22 ± 0.06 ka, as best reflecting emplacement of the boulder, while the sedimentary pIRIR225 signal was probably incompletely bleached.

The 4.2 ka age for the cobble emplacement is consistent with the ages for other nearby stone structures, but significantly underestimates the expected age for a Rodedian site of ca. 9–7 ka (Avner et al. 2014). The authors argue that this may be due to a later intervention at the site in the late 3rd millennium BC that would presumably have involved moving the cobbles. This scenario would be consistent with the presence of an earlier, undatable exposure and burial event identified in the luminescence-depth profiles from the cobble.

Dating the Khatt Shebib megalithic structure in Jordan (al Khasawneh et al., 2019a)

Key takeaways

- Aim: Use rock surface burial dating to provide the first direct ages for the Khatt Shebib megalithic structure, a 150-km-long linear, dry stone structure of unknown purpose in Jordan.
- OSL-depth profiles were modelled and $L_1(x)/L_2(x)$ method introduced as a simple and elegant way to assess whether, and how deeply a rock surface was sufficiently bleached prior to burial.
- Well-bleached layers identified and used to determine a burial date of 400 ± 100 BCE, indicating construction of this section of the Khatt Shebib during the Iron Age.

Description

Khatt Shebib is a 150-km-long linear stone structure in Jordan that comprises mostly piled locally available rocks with occasional sections of formally built wall. The purpose and age of the structure are unknown, with the only chronological hypotheses being based on Iron Age and Roman period pottery nearby sections of the structure.

Two emplaced sandstone cobbles (~ 30 cm \times 30 cm \times 20 cm) that were collected from the structure yielded a well-behaved, fast-component dominated OSL signal. Five to six cores (10–25-mm diameter, 15–30-mm length) were collected from the buried surfaces of each cobble and sliced at ~ 1 -mm thicknesses. Slices were disaggregated using hydrofluoric and hydrochloric acid and grains were measured as multi-grain aliquots: four aliquots were measured for each slice to obtain L_n/T_n values, with an additional six aliquots being measured to determine D_e values from the first five slices.

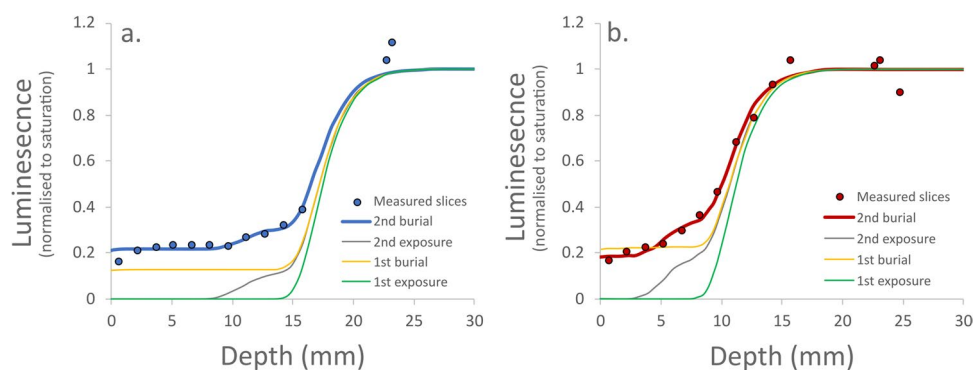


Fig. 8 Luminescence-depth profiles for IR50 (a) and pIRIR225 (b) measurements from a paving cobble at a Rodedian site in Israel. Data points show L_n/T_n values for each slice into the surface, solid lines show the data fitted with the Freiesleben et al. (2015) model, and

dashed lines show the resulting predicted profiles for multiple burial and exposure events obtained from the model. See text for details. Modified from Sohbaty et al. (2015)

OSL-depth profiles show intra-cobble variability of up to 3 mm in the depth of the bleaching front for each cobble, suggesting to the authors that the rock surfaces had not been uniformly light exposed before construction. Likewise, one cobble (KS1) appears to have been better bleached than the other (KS2). To investigate further, OSL-depth profiles were fitted with the Freiesleben et al. (2015) model, assuming that the light attenuation factor (μ), the average excitation rate ($\overline{\sigma\varphi_0}$), and D_0 were common to all cores from each rock. The authors fitted their OSL-depth profiles with two models: one assuming only one exposure event ($L_1(x)$) and the other assuming an exposure and burial event ($L_2(x)$). To assess how well and how deep each core was bleached, the authors devised a simple approach; they calculated the ratio of $L_1(x)/L_2(x)$ over the length of the cores. A slice was considered sufficiently well-bleached if $L_1(x)/L_2(x)$ yielded a value < 0.03 , indicating that that slice had been buried with an unbleached luminescence signal less than 3% of the signal that later developed during burial (Fig. 9).

De estimates were calculated using the SAR procedure for aliquots from the layers identified as having been well-bleached prior to burial. Three cores from cobble KS2 were too poorly bleached; even the surface 1 mm was affected by partial bleaching (Fig. 9b). The other three cores from KS2, however, yielded sufficiently-bleached surface slices to yield a burial age of 2.39 ± 0.05 ka for the surface. All cores from cobble KS1 were well bleached to a depth of at least 4 mm (Fig. 9a), yielding a burial age for the surface of 2.45 ± 0.13 ka. The samples yielded an average burial date of 400 ± 100 BCE, providing the first direct ages for the Khatt Shebib megalithic structure and indicating an Iron Age construction date for this section.

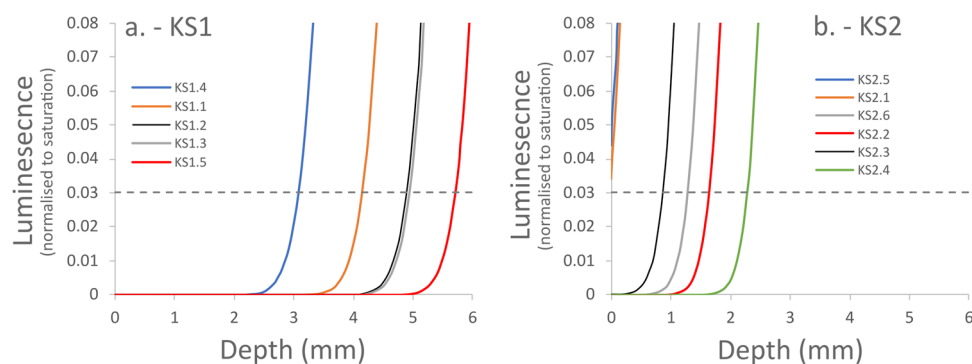


Fig. 9 Luminescence-depth profiles from two emplaced sandstone cobbles from the Khatt Shebib were fitted with the Freiesleben et al. (2015) model twice—once assuming only one exposure event ($L_1(x)$) and once assuming an exposure and burial event ($L_2(x)$). Ratios of

Dating a desert hunting trap (kite) stone structure in Jordan (al Khasawneh et al. 2019b)

Key takeaways

- Rock surface burial dating was used to provide first direct ages for a pit that is part of the Jibal al-Gadiwiyt desert kite stone structure construction and use.
- Well-bleached layers that retain a burial signal were identified in rock surfaces and used to calculate burial ages for a series of stratigraphically related stone surfaces.
- Stone surfaces that reflected pit construction and those that reflect pit back-filling yielded consistent burial ages of ~ 9.8 ka, indicating Neolithic construction and only a brief period of use before maintenance ceased.
- Brief structure-use was corroborated by small OSL-exposure age (~ 4 years) from wall of pit.

Description

The Jibal al-Gadiwiyt kite (Jordan) is a desert kite stone structure that comprises two long stone walls converging at a polygon-shaped enclosure that is surrounded by small stone circles that likely served as hunting hides. Despite their ubiquity across the Middle East and Central Asia, almost no ages exist to indicate when these structures were constructed or used. Excavations at Jibal al-Gadiwiyt revealed that the circular hunting hide structure is a 1.3-m-deep pit lined with stones that had been back-filled over time by water-lain and aeolian sediments.

Three stone samples were collected for OSL rock surface burial dating, including a stone from the wall of the hide that had been laid down during construction (sample E24), one surface of which (surface *I*) had been exposed for 5 months

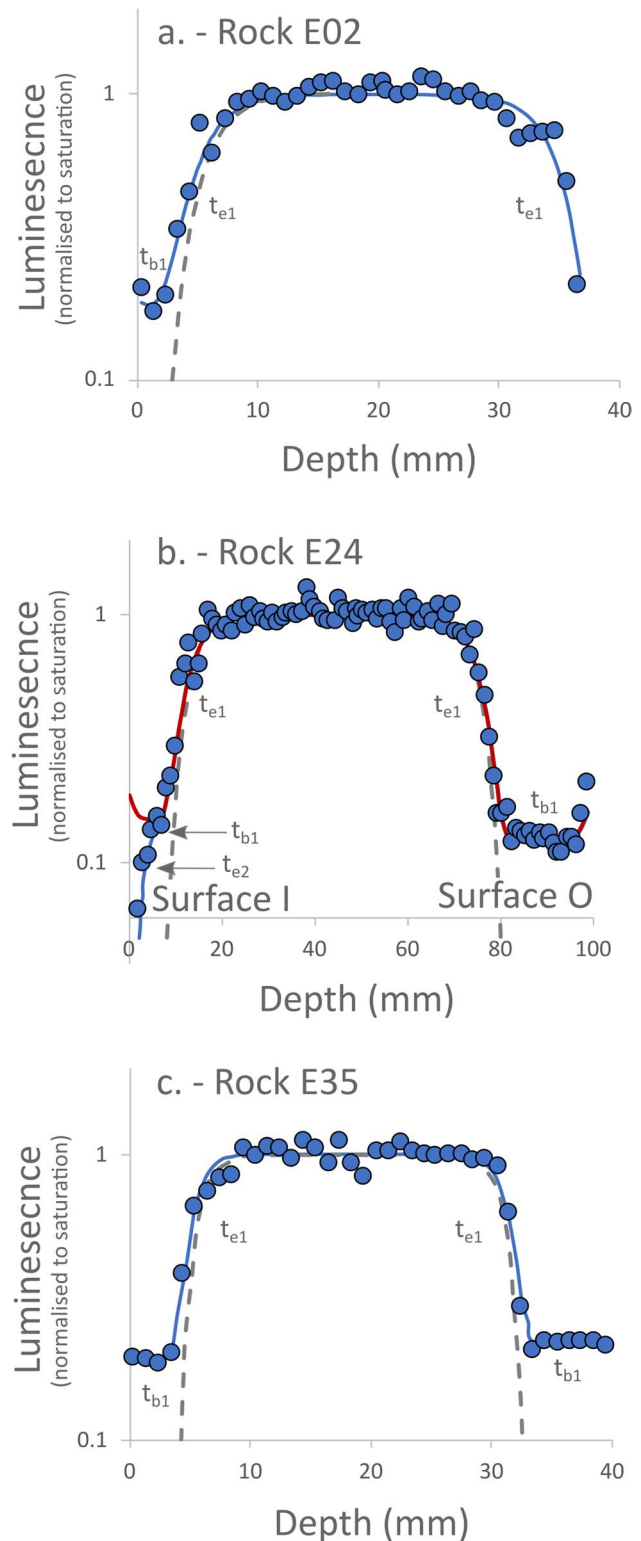
the model fits $L_1(x)$ and $L_2(x)$ for each core, represented as different coloured curves, are shown (**a** KS1 and **b** KS2). A $L_1(x)/L_2(x)$ ratio < 0.03 (dashed line) indicates that the slice had been well bleached prior to burial. Modified from al Khasawneh et al. (2019a)

Fig. 10 Luminescence-depth profiles for three rocks from a hunting hide at the Jibal al-Gadiwiyt kite in Jordan: Rock E02 (a), rock E24 (b), and rock E35 (c). Blue data points are L_n/T_n values calculated for slices, solid blue lines are the result of fitting the Freiesleben et al. (2015) model to the data, dashed grey lines are the predicted profiles after the earliest exposure event, and the red line is the predicted profile after the first burial event. Rocks E02 and E35 and surface O of rock E24 could best be described by one exposure and one burial event, while rock E24 surface I could best be described by one exposure, one burial, and a subsequent exposure event. Modified from al Khasawneh et al. (2019b)

prior to sampling, while the other surface (surface O) had remained buried, presumably since construction of the pit. The remaining two cobbles were collected from the floor of the pit (E02) and from the back-fill (E35). These two samples are stratigraphically younger than E24 and could have been put in place by natural events during the back-filling of the pit. Cobble surfaces were drilled (25–50-mm length) and sliced in 1-mm increments. Slices were disaggregated using hydrofluoric and hydrochloric acid and grains were measured as multi-grain aliquots. A fast component dominated OSL signal that performed well in dose recovery experiments was measured.

OSL-depth profiles were modelled following Freiesleben et al. (2015). Samples E02 (Fig. 10a) and E35 (Fig. 10c) and surface O of E24 (Fig. 10b) were fitted using a model described by one long exposure and a subsequent burial event. Sample E24 surface I was fitted using a model described by one long exposure, a subsequent period of burial, followed by a second exposure event, which would describe the five months of exposure following excavation but prior to sampling (Fig. 10b). The modelling results and the $L_1(x)/L_2(x)$ approach was used to identify those layers that had been well bleached prior to burial and, for surface I of E24, not affected by the post-excitation period of exposure.

De estimates for burial age calculation were measured using the SAR procedure for aliquots from the layers identified as having been well-bleached prior to burial. Rock E24 yields consistent burial ages of 8.6 ± 0.7 ka for surface O and 9.7 ± 1.2 ka for surface I, suggesting that pit was not used for very long. This is supported by the burial ages for rocks E02 (9.8 ± 0.2 ka) and E35 (10.8 ± 1.1 ka). The statistical consistency of burial ages for E24 (surface O), which reflects construction of the pit wall, with those for E24 (surface I), E02, and E35, which reflect refilling of the pit with sediments, indicates that the pit could not have been maintained for more than a few hundred years after construction. This is further supported by an OSL-exposure age for rock E24 (surface I), calibrated using the 5-month exposure time after excavation but before sample collection, which indicated an exposure duration on the order of years



between pit construction and the subsequent pit backfilling buried the surface.

Using this combined approach of rock surface burial and exposure dating of multiple, stratigraphically related rocks

from the Jibal al-Gadiwiyt kite structure, it could be determined that the structure was constructed $\sim 9.8 \pm 0.8$ ka during the Neolithic and was only used for a very short duration before the pits ceased to be maintained.

Dating a Bronze Age dry stone structure in the Italian Alps (Ageby et al. 2021)

Key takeaways

- Here, rock surface burial dating and luminescence-depth profile modelling of buried gneiss cobbles were used to date buried Early and Middle Bronze Age archaeological deposits in a dry-stone structure.
- Luminescence-depth profiles were used to identify well-bleached slices from surfaces, yielding robust age estimates for the most recent phase of cobble surface exposure and burial. Complex site geomorphology is reflected in cobble age estimates. One cobble was buried during a period of glacial advances and retreats during deglaciation prior to its incorporation into the structure. The remaining cobbles somewhat underestimate the archaeological deposit ages (derived from radiocarbon estimates), suggesting that they were not completely buried by colluvium until hundreds to a thousand years after human activities had ebbed.
- IRSL50 luminescence-depth profiles and pIRIR290 measurements from one cobble show that it had been heated to > 550 °C, despite no visual indications of heating. The IRSL50 and pIRIR290 age estimates indicate a Late Bronze Age/Iron Age antiquity for the heating event, generally agreeing with the chronostratigraphic model derived from the radiocarbon chronology and rock surface burial dating estimates.

Description

The study area consists of a partly buried dry-stone wall that likely served as a livestock enclosure at ~ 2240 m above sea level in the Italian Alps. Excavations uncovered a ~ 40 -cm-thick deposit with two archaeological units, US4a and US5a, which contained archaeological materials including knapped chert artefacts and potsherds. The archaeological units were separated by and capped by colluvial deposits. Radiocarbon ages of charcoal fragments indicate that US5a dates to the Early Bronze Age (~ 2200 – 1500 BC), while US4a has a more complex chronology, with ages ranging from the Middle Bronze Age (~ 1500 – 1400 BC) to 537–654 and 426–596 AD.

Two paragneiss cobbles from each archaeological unit were sampled for luminescence rock surface burial dating. Cores were drilled and sliced using standard procedures, and a low-temperature pIRIR150 signal was measured during SAR sequences. Cobble burial ages were estimated by

measuring IR50 De values from slices at depths into the rock surface that had been exposed to sufficient sunlight to be reset before burial. They identified well-bleached slice depths following the $L_1(x)/L_2(x)$ approach of al Khasawneh et al. (2019a). All ages were corrected for fading.

Luminescence-depth profiles showed that all cobbles had bleached luminescence signals at their surfaces. However, there was some variability in the depth of resetting between cores from the same surfaces and between different cobbles and surfaces. Fitting of the depth profiles with the model of Freiesleben et al. (2015) and visual inspection indicated that at least one surface from each of the four cobbles was sufficiently bleached and retained a luminescence-depth plateau that could yield an age for the most recent burial event.

One sample from US5a yielded an age of 18 ka, reflecting exposure and subsequent burial during the glacial retreats and advances following the Last Glacial Maximum. The remaining ages need to be considered in the site's geomorphological context, namely that the dated cobbles would have sat protruding from an archaeological deposit before being buried by colluvium later. The up-facing surface of a sample from US5a yielded an age of 1460–720 BC, which is slightly younger than the Bronze Age radiocarbon chronology for these deposits. The authors suggest that this cobble surface slightly protruded from the colluvium that overlaid US5a, thus continuing to bleach for several centuries before subsequent burial. The two cobbles from US4a significantly underestimate the expected Late Bronze Age dates indicated by radiocarbon of charcoal, yielding ages of 890–1150 AD (MZ051S-2 top), 550–810 AD (MZ051S-3 top), and 880–1060 AD (MZ051S-3 bottom). The authors conclude that US4a was likely deposited during the Late Bronze Age or Iron Age, based on the radiocarbon results. The US4a deposits then remained exposed for up to 1000 years, before the reactivation of the nearby hillslopes (possibly due to human land use in the Early Middle Ages) buried the deposit in colluvium towards the end of the 1st millennium AD/beginning of the 2nd millennium AD.

A fascinating benefit of using the luminescence rock surface dating approach was that a heating event of one of the cobbles could be identified despite no visual indications of previous heating. One sample from US4a (MZ051S-2) reached only very low L_n/T_n values in the centre of the cobble (much lower than field saturation), despite the cobble being ~ 70 mm thick. To allow a comparison of two signals with very different bleaching and fading characteristics, several slices from deep within the cobble were measured using a pIRIR290 SAR protocol, which yielded results that were also not in field saturation. Given that the pIRIR290 and IR50 signals could be reset by heating up to ~ 550 °C and that optically resetting of both signals ~ 45 mm into the paragneiss would not be possible, the authors inferred that the cobble had been heated to > 550 °C for long enough to reset the luminescence signal up to 45 mm into the cobble (Fig. 11). The fading-corrected IR50 age and the pIRIR290 ages for the heating event were consistent,

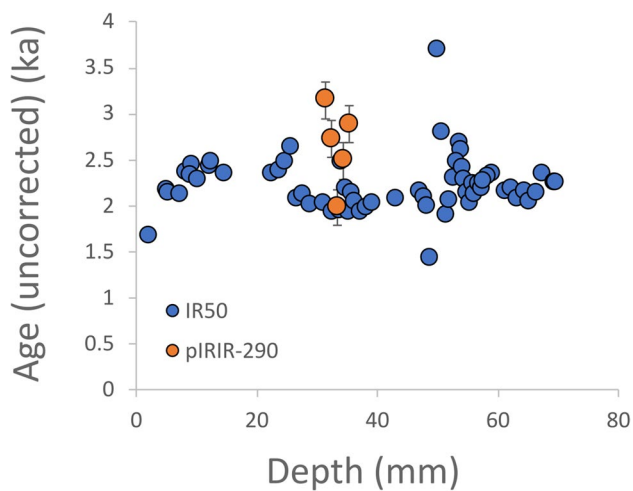


Fig. 11 IR50 (blue) and pIRIR290 (orange) slice ages calculated throughout a cobble from a dry stone structure in Italy (sample MZ051S-2). The plateau between 5 and 70 cm is not in saturation, indicating signal resetting throughout the cobble. The depth of resetting and the agreement between IR50 and pIRIR290 ages suggests the cobble had been heated to very high temperatures between 2.64 ± 0.75 ka and 3.03 ± 0.67 ka. Modified from Ageby et al. (2021)

being 2.64 ± 0.75 ka (1370 BC–130 AD) and 3.03 ± 0.67 ka (1680–340 BC), respectively. The authors infer that this rock experienced an anthropogenic heating event, such as inclusion in a hearth, during the Late Bronze Age or Iron Age, thereby supporting the chronostratigraphic interpretation of US4a despite the complex cobble burial age estimates from the unit.

Dating Iberian rock art (Moayed et al. 2023)

Key takeaways

- Aim: Use luminescence rock surface burial dating to date a rockfall event that can temporally constrain a panel containing two rock art styles: Levantine (made before the rockfall) and Schematic (made after the rockfall).
- Luminescence-depth profiles were analysed following the approach of Rades et al. (2018) to identify that only the IR50 signal from one of three rockfall boulders was sufficiently bleached to yield a reliable burial age for the block, and therefore the timing of rockfall.
- Surface slice of block PE2.2 yielded a fading-corrected IR50 age of 2.7–2.9 ka, indicating that the Schematic rock art was produced during the end of the Late Bronze Age.

Description

Similar to Chapot et al. (2012) and Pederson et al. (2014), Moayed et al. (2023) aimed to provide temporal constraints

to a panel of rock art by using a luminescence rock surface burial dating approach to date a rockfall event. In this case, the rockfall had affected a panel that contained two different rock art styles (the Levantine and Schematic styles) at a sandstone site in eastern Spain. The part of the panel with Schematic rock art was exposed following a rockfall event, which removed a block that had constrained the location of the Levantine rock art. Therefore, dating the rockfall event could provide a maximum age for the Schematic rock art and a minimum age for the Levantine rock art.

Three talus blocks at the base of the rock art panel were determined to have been part of the rockfall event and were sampled (PE2.2, PE2.3, and PE2.8) along with samples from the underlying sediments. Given that they were concealed from light at the same time, the three boulders should thus have the same luminescence burial age. A fourth sample (PE2.10) was collected from the exposed side of one of the blocks to investigate the bleaching processes of the lithology.

In the laboratory, the block samples were cored, sliced (1.5-mm-thick slices), and the slices were broken into chips that were mounted in stainless steel cups for measurement using a pIRIR225 SAR protocol. IR50 dose recovery experiments demonstrated a small residual dose (1.67 Gy) and acceptable measured/given dose ratios (0.90 ± 0.04). Typical luminescence-depth profiles from buried samples could be measured for all samples' IR50 signals and only one sample's (PE2.2) pIRIR225 signal. The approach of Rades et al. (2018) indicated that the IR50 signal from sample PE2.2 was sufficiently bleached beyond the 1.5-mm thickness of the first slice, while all other samples and signals were not sufficiently bleached. Consequently, an IR50 age was calculated for the first slice of sample PE2.2, which was corrected for anomalous fading using two methods that yielded consistent fading-corrected ages of 2.7 ± 0.5 ka (*g*-value factor—Auclair et al. 2003; Huntley and Lamothe 2001) and 2.9 ± 0.3 ka (field to laboratory saturation ratio—Rades et al. 2018) for the timing of the rockfall event. They conclude that the Schematic rock art must have been made after 2.9 ka, which is evidence for the presence of Schematic rock art traditions from the end of the Late Bronze Age.

Summary of archaeological applications

These examples of luminescence rock surface dating provide evidence for how these new approaches can supplement more conventional dating methods (e.g. OSL dating of sediments and radiocarbon) as well as dating previously difficult contexts due to the absence of organics or other dateable material. Luminescence rock surface dating has been used to:

- date rockfall events from panels containing rock art, thereby providing temporal constraints on said rock art (Chapot et al. 2012; Sohbaty et al. 2012a; Pederson et al. 2014; Moayed et al. 2023);
- develop a chronology for discard and post-depositional movement of lithic artefacts at an artefact scatter site (Gliganic et al. 2021); and
- date the construction of a range of previously un-datable rock-based archaeological features, including:
 - a whetstone (Freiesleben et al. 2015),
 - a pavement (Sohbaty et al. 2015),
 - a hunting trap structure (al Khasawneh et al. 2019b),
 - a branch of a megalithic stone structure (al Khasawneh et al., 2019a), and
 - a dry stone wall (Ageby et al. 2021).

Some unique benefits that are available when using a luminescence rock surface dating approach in appropriate settings with appropriate lithologies include:

- direct age constraints on lithic archaeological materials and features several orders of magnitude larger in size compared to the sediments that build up the substrate in which these archaeological features are encased (i.e. sand to silt sized mineral grains). Up to now, the age for most of these lithic archaeological materials could only be constrained indirectly by dating these associated mineral grains or proximal organic material via sedimentary luminescence or radiocarbon dating;
- identifying pre-burial bleaching in luminescence-depth profiles, allowing the assessment of whether the surface had been exposed to sufficient sunlight to bleach the pre-existing luminescence signal;
- dating the exposure of currently exposed or recently buried rock surfaces on a temporal and spatial scale that compliments cosmogenic nuclide-based exposure dating; and
- identifying multiple burial and exposure events in a luminescence-depth profile, thereby allowing a reconstruction of exposure and burial history of a rock surface.

Caveats, obstacles, and open questions

While luminescence rock surface dating approaches have great potential, they are still in development and, thus, open questions about the method remain. In the following, we identify some necessary considerations when assessing whether a luminescence rock surface dating approach

would be appropriate. As we shall see, most of these caveats relate to rock surface exposure dating, while rock surface burial dating is a more straightforward undertaking.

Lithology

The rocks that are being targeted for dating must contain minerals that have a usable luminescence signal, such as quartz or K-feldspar. However, the luminescence properties of these minerals tend to vary between different lithologies, albeit in a broadly systematic way, making some rock types more suitable for a rock surface dating approach than others. Some rock types, such as limestones, which are dominated by carbonate minerals do not yield bright or stable optically stimulated luminescence signals, making rock surface dating on carbonate lithologies challenging as a routine technique (Galloway 2002; Liritzis et al. 2010). While quartz from sedimentary and meta-sedimentary rocks can yield a bright and stable OSL signal, quartz derived from igneous and metamorphic (i.e. crystalline) rocks tends to yield dim and unstable OSL signals (Jeong and Choi 2012; Chapot et al. 2012; Feathers et al. 2019; Gliganic et al. 2021; Alexanderson 2022). Hence, for crystalline rocks, the feldspar IRSL signal is often exploited because this signal is typically much brighter than the quartz OSL signal in igneous and metamorphic lithologies (e.g. Jenkins et al. 2018; Feathers et al. 2019). The downside of the IRSL signal is that it tends to be more difficult to bleach (Godfrey-Smith et al. 1988; Colarossi et al. 2015) and likely exhibits anomalous fading that needs to be corrected for (Huntley and Lamothe 2001). A similar situation is encountered in many volcanic rocks, which typically exhibit no or very dim quartz OSL signals unsuited for dating, but reasonably bright IRSL signals. For example, Feathers et al. (2019) applied luminescence rock surface burial dating to fine-grained volcanic rocks that were part of a geoglyph in Peru. A quartz OSL signal was not detectable, while the non-fading pIRIR signal from the slices was not sufficiently bleached and the IR50 signals were dim and suffered from anomalous fading. Still, they determined fading-corrected IR50 burial ages, which enabled some chronological constraints for the geoglyph with the caveats that partial bleaching and anomalous fading may have impacted the accuracy of the ages.

Furthermore, the rock-type must also be reasonable translucent or of a light colour in order to allow a luminescence-depth profile to be developed within a reasonable amount of geologic time. Ou et al. (2018) investigated how light is attenuated in different rock types (greywacke, sandstone, two granites, and quartzite). In addition to a sunlight bleaching experiment, they directly measured the light attenuation in rock slices using a spectrometer. They showed that

the luminescence signals from different rock types can be bleached to different depths for a given light exposure. Lighter coloured rocks attenuated light less (i.e. allowed more light to pass through) and were bleached to deeper depths than darker coloured rocks.

Given that different coloured rocks or mineral aggregations within a rock attenuate light at different rates, it logically follows that the target rocks should be as internally homogeneous as possible. Rock coatings, weathering rinds, staining, and varnish, as well as internal foliations, iron precipitates, and millimetre-scale heterogeneity in mineral colour within the rock, may affect how light penetrates the rock surface. Meyer et al. (2018) measured luminescence depth profiles for whole slices of metamorphic granite gneiss and quartzite samples, then quantified the colour of each slice using a scanner and an RGB quantification approach. They showed clearly that the RGB value (i.e. colour) is strongly correlated with the position of the bleaching front in the luminescence-depth profile. One example was from three quartzite rock surfaces with identical exposure ages (1.6 years) and locations. Two of the surfaces were bleached to a depth > 10 mm, while one (TIN2016-150) was bleached to a depth of only ~3 mm. The RGB-depth plots clearly show a sharp drop in the RGB profile at the shallow bleaching front (i.e. excursion to darker values; Fig. 12), corresponding to a thin, millimetre-scale band of iron hydroxide staining present in that rock sample that was not visible until the cores were collected. It was determined that the dark iron staining prevented light penetration in sample TIN2016-150, resulting in a significantly shallower OSL-depth profile. This, however, is not always problematic. Ageby et al. (2021) performed a bleaching experiment comparing luminescence-depth

profiles for surfaces that were bleached perpendicular to vs parallel to opaque foliations in their paragneiss rocks. They did not observe a significant difference between the two orientations and suggested that mineral-scale heterogeneity had little effect on their samples. However, in the absence of a slice specific quantification of the RGB values on a core by core base, such conclusions must be evaluated with care and maybe indicate that the opaque foliation in the samples of Ageby et al. (2021) was not pervasive but rather fibrous or knotty allowing light to still penetrate in a quasi-isotropic manner.

Another form of mineral-scale heterogeneity was observed by Meyer et al. (2018). The granite gneiss samples often yielded wildly scattered luminescence-depth profiles that varied in shape and bleaching depth between different cores from the same surface. They observed that opaque mineral phases formed large, ~centimetre scale aggregates that occur in ‘patches’, rather than planar layers in the granite gneiss samples. The RGB, XRD, and luminescence-depth profiles indicate that these patches may ‘shadow’ the constituent mineral grains at deeper depths causing the observed noise in the luminescence-depth profiles and that the efficiency of light ‘piping’ around these dark patches via a (semi)continuous network of more transparent mineral phases (such as feldspar and quartz) is likely to be important (Meyer et al. 2018). This level of mineralogical heterogeneity may preclude surface exposure dating if cannot be controlled for.

Furthermore, the occurrence of radioactive hot spots within a host rock and the distribution of these hot spots relative to the drill core position can have a significant effect on the spatially resolved dose rate and De values, hence on the smoothness and shape of luminescence-depth profiles and age-depth profiles. Such hot spots might be composed of zircon, rutile, or other types of heavy mineral grains with high internal radionuclide concentrations or of interstitial kaolinite (i.e. a potassium bearing clay mineral forming diagenetically along grain boundaries in pore spaces). In crystalline host rocks such as gneisses or granites, zircon or rutile are common accessory minerals (Meyer et al. 2018), but even in pure quartzite lithologies such as those investigated by Gliganic et al., (2021), heavy mineral concentrations can occur. In the latter case, recognition of these hot spots and dose rate anomalies was important and thus sample specific dose rate calculations ultimately resulted in a better resolved chronology. It is therefore worthwhile to accompany any rock surface dating campaign with a proper petrographic investigation of the sampled rock type and eventually follow-up with mineralogical and chemical qualitative and quantitative analysis.

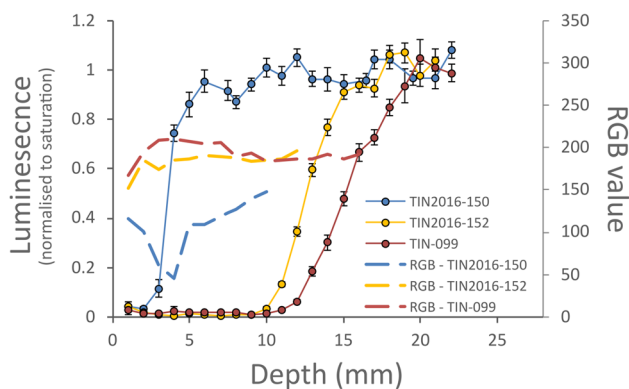


Fig. 12 OSL-depth profiles (data points and solid lines) and RGB profiles (dashed lines) from three quartzite samples from the same location with the same known exposure duration (1.66 years). RGB and OSL-depth profiles are colour coordinated for each sample. The RGB axis quantifies the colour of each slice and ranges from 0 (black) to 255 (white). RGB values were measured for slices from a core collected adjacent to its corresponding OSL-depth profile. Note that bleaching depth correlates with changes in RGB values. See text for details. Modified from Meyer et al. (2018)

Erosion

Rock surface erosion is another consideration that can complicate luminescence exposure dating. If erosion is not taken into account, the luminescence-depth profile will appear to

be too shallow and thus result in an underestimated exposure age (Sohbati et al. 2018; Lehmann et al. 2019). Sohbati et al. (2018) leveraged this observation and developed an approach to quantify erosion rates using luminescence-depth profiles in equilibrium. Lehmann et al. (2019) expanded on this to pair luminescence-depth profiles with terrestrial cosmogenic nuclide (^{10}Be) exposure dating to quantify both exposure ages and erosion rates for glacially polished bedrock surfaces. Freiesleben et al. (2022) modelled the effects of erosion on luminescence-depth profiles and the apparent exposure age relative to the true exposure age. They showed that the effects of erosion on the luminescence-depth profile always outweigh the effects of improved bleaching as the rock surface is lowered, resulting in an underestimated apparent OSL or IRSL rock surface exposure age. Higher erosion rates for a given true exposure age result in increasingly underestimated apparent exposure ages. Likewise, longer true exposure durations with a constant erosion rate also result in lower apparent exposure ages.

Insolation

The way light interacts with the rock sample is a fundamental consideration, particularly when it comes to choosing a calibration sample for luminescence rock surface exposure dating. Is there a difference in bleaching between north and south facing surfaces? Is there a difference in bleaching between horizontally and vertically oriented faces? How do these differences in insolation and incidence angle manifest over the course of an entire year?

Fuhrmann et al. (2022) performed an experiment using granite (IRSL) and sandstone (OSL) samples. They varied the orientation of samples while controlling the exposure duration, directly measuring the photon flux at the rock surface using pyranometers, and modelling the incidence of light to each surface over the study to determine the influence of spatial orientation of a rock surface relative to the sun on the bleaching depth. Their results confirmed that the opacity of the rock and the total insolation significantly affect bleaching depth, with higher insolation resulting in better bleaching. They also observed that the incidence angle at which light interacts with the rock surface strongly influenced the depth of the luminescence-depth profiles—higher incidence angles (i.e. perpendicular to the rock surface) bleached rock surface more efficiently than low incidence angles for a given total insolation. This result suggests that the effectiveness of bleaching in a given rock surface will change throughout the year due to seasonal changes in the sun's path across the sky. These changes in seasonal insolation would have a much larger effect on the depth of luminescence-depth profiles for younger surfaces (e.g. experimentally created calibration surfaces with an age on the order of months to years) than for older surfaces (e.g.

target unknown age surfaces with an age on the order of decades to millennia). Therefore, they concluded that ideal calibration samples should be of the same lithology, in the same location, and have the same orientation as the unknown age sample. Likewise, calibration samples should be collected in year increments so that seasonal differences in solar incidence angle and bleaching effectiveness for a given surface would not bias the calibration. Alternatively, calibration samples could be old enough for seasonal differences to be inconsequential.

Surface exposure dating model

There is also room for improvement in the models that describe bleaching into a rock surface for luminescence surface exposure dating (e.g., Sohbati et al. 2012a; Freiesleben et al. 2015, 2022). These models assume that the daylight spectrum does not change significantly with depth into the rock, thereby allowing the assumption that the attenuation factor (μ) can be treated as a constant. However, even Sohbati et al. (2012a) discuss that the shorter wavelengths of the solar spectrum are absorbed faster than longer wavelengths, indicating that the bleaching spectrum changes with depth. The spectrometer measurements reported by Ou et al. (2018) explicitly show this, indicating that shorter wavelengths (~400 nm) are more attenuated than longer ones in rock slices.

Recently, Freiesleben et al. (2022) developed a new analytical expression for fitting luminescence-depth profiles in rocks based on a general order kinetic model (McKeever and Chen 1997), which improves the accuracy of age estimates for IRSL and pIRIR profiles. The authors also demonstrated that calibration with a single known-age sample, as common practice in rock surface exposure dating (e.g. Sohbati et al. 2012a; Gliganic et al. 2019), often gives inaccurate ages regardless of the chosen model order, unless the age of the calibration profile is of the same order of magnitude as the age of the unknown profile. They suggest an alternative method of exposure dating called an exposure response curve (ERC) method, which bypasses the complexities and uncertainties associated with model parameter calibration. In this approach, an ERC is constructed by plotting the inflection point of the luminescence-depth profiles (i.e. the depth at which the L_x/T_x signal has reached ~50% of its saturation level) from a series of known age surfaces (including samples that are older and younger than the target surface) as a function of the natural logarithm of the known ages. The inflection point of the unknown age surface can then be interpolated onto the ERC to determine its exposure age. However, Freiesleben et al. (2022) concede that the requirements of this approach, namely the presence of at least two known-age samples that bracket the age of the target sample, are unlikely to be commonly available.

Rock surface exposure versus burial dating: summary of caveats, obstacles, and open questions

The caveats listed above are not meant to dissuade future use of the developing methods of luminescence rock surface burial and exposure dating. On the contrary, a close read of the caveats reveals that the majority of the major roadblocks mainly affect rock surface exposure dating and this is precisely why efforts are currently focusing on methodological improvements of the exposure aspect of rock surface dating (e.g. Meyer et al. 2018; Gliganic et al. 2019; Fuhrmann et al. 2022; Sellwood et al. 2019; Sellwood et al. 2022; Freiesleben et al. 2022). Luminescence rock surface burial dating on the other hand is on comparatively steady methodological footing. Table 2 outlines the relevance of the various complicating considerations discussed in this section to the luminescence rock surface burial dating and exposure dating methods.

While all aspects have significant implications for, and could limit the successful utilisation of, the exposure dating approach, most are irrelevant for or can be circumvented for successful burial dating. Hence, in the following, each of the caveats listed in Table 2 is briefly discussed with respect to rock surface exposure versus rock surface burial dating, and their methodological relevance and broader implications for dating applications are highlighted:

- The rocks of interest clearly require a lithological composition that encompasses a sufficient number of minerals that emit an OSL or IRSL signal that is bright and stable for any luminescence-based dating techniques to be possible.
- Translucency of the rock surface is paramount for both luminescence rock surface exposure and burial dating approaches. If a rock is too dark to allow sufficient light penetration, then it is unlikely that bleaching will occur to enable successful burial or exposure dating.

- For successful rock surface exposure dating, the rock texture must be homogeneous enough with respect to translucent mineral grains to allow sunlight to penetrate into the rock interior in a quasi-isotropic (i.e. in all directions homogenous) way in order to generate a well-defined and reproducible luminescence-depth profile for subsequent age calculation. For burial dating, this pre-requirement of isotropy is much less of an issue, because if the surface slice or slices are bleached, a burial age can be determined by measuring the reaccumulated dose. However millimetre-scale dose rate heterogeneity could result in significant differences in the dose rate experienced by given slices, and this difference would not be identified in the dose rate modelling. This could lead to scattered and misleading age-depth profiles, which could result in spurious burial ages. That being said, it could be possible to (i) identify the effects of millimetre-scale dose rate heterogeneity in the age-depth profile data as a lack of plateaus and—as outlined above—(ii) for aberrant or complicated rock samples, the use of petrological techniques such micro XRF, microprobe, or thin-section analysis would help to identify and tackle the effect of lithological heterogeneity on the microscopic level.
- High rock surface erosion rates would remove portions of the rock surface and result in inaccurately young exposure ages. Perniciously, this issue may not be able to be recognised as a problem in the data. However, with regard to burial dating, surface erosion (i) is less likely to affect buried surfaces, (ii) would not inhibit identification of age-depth plateaus to determine burial ages as long as bleaching was sufficient prior to burial, and (iii) would be clear in the data if erosion had eradicated the entire age-depth profile.
- While the specific insolation conditions should be as close as possible for the calibration surface and the target surface in rock surface exposure dating, the insolation conditions do not matter for burial dating, so long as the surface was exposed to sufficient sunlight prior to burial—an aspect that can be clearly seen in the luminescence-depth profiles (e.g. al Khasawneh et al., 2019a).
- The specifics of the surface exposure dating model has little relevance for successfully applying a rock surface burial dating approach, which can be undertaken by calculating age-depth profiles, thereby avoiding any modelling uncertainties.

Table 2 Relevance of the caveats and obstacles discussed above to the luminescence rock surface burial dating and exposure dating methods

Consideration:	Burial dating	Exposure dating
Lithology		
Luminescence signal presence and stability	x	x
Translucency	x	x
Homogeneity of rock texture	~	x
Erosion		
		x
Insolation		
		x
Surface exposure dating model		
		x

Potential applications and future directions

The infancy of luminescence rock surface dating methods means that there are still many potential applications that are yet to be fully realised. Below is a brief discussion of some difficult-to-date site types and archaeological contexts

that could benefit from a luminescence rock surface dating approach.

Direct dating of artefact discard

One common source of disagreement regarding chronologies for archaeological sites is that the lithic artefacts are not being directly dated, but are instead stratigraphically associated with dated materials (e.g. charcoal or buried sand grains dated with radiocarbon or luminescence dating, respectively). As such, there is the possibility that post-depositional mixing of artefacts and/or sediment grains by bio- or pedoturbation could result in spurious associations between artefacts and the dated media (Leigh 1998; Balek 2002; Peacock and Fant 2002; Gliganic et al. 2016). One way to mitigate this risk is by directly dating the lithic artefacts themselves with a luminescence rock surface burial dating approach. Lithic artefacts and surrounding sediments could be excavated and collected in a light-safe way (e.g. at night or under a lightproof tent). By constructing luminescence age-depth curves through the artefacts, a sunlight exposure and burial history of the artefacts can be reconstructed, allowing a direct estimate of the burial age of the artefact. Some potential benefits of using this approach would be the ability to directly date the burial of artefacts themselves and an explicit test of whether the artefacts had been completely bleached before burial. Some potential complications with this approach would be that (i) the lithic artefacts would need to be of a lithology with a reasonably well-behaved luminescence signal, such as quartzite; (ii) the artefact lithology would need to reveal proper bleaching properties (i.e. sufficient translucency) in order for a measurable bleaching-with-depth profile and eventual subsequent burial signal in the form of a De plateau to be recorded; and (iii) the artefacts would need to be physically impacted by drilling and slicing, which would likely require complex regulatory approvals to be obtained.

A further site type that could benefit from a rock surface dating approach are surface artefact scatter sites. Such sites are common in the archaeological record and can yield information about how humans produced lithic technologies, moved around and utilised the landscape, and exploited resources through time. However, these globally ubiquitous types of sites are found on the land surface and thus have limited stratigraphic associations with datable materials. Where sites are not buried, typological and stylistic associations between tool types or art motifs are often cited, though this approach (i) requires significant assumptions, (ii) is untestable, and (iii) may be unreliable. Huge pools of potential knowledge are, thus, ignored from sites that are on the land surface and thus lack a dateable stratigraphic context. As discussed in the ‘Case studies’ section, Gliganic

et al. (2021) used a luminescence rock surface burial dating approach to date six lithic artefacts on the surface at an artefact scatter site in Tibet. While they were able to reconstruct a history of site use and environmental change, more dated artefacts would certainly have yielded a higher resolution record. Consequently, future studies could aim to measure tens of artefacts from a given site to reconstruct a high-resolution record of artefact discard and post-depositional movement at the sites. This kind of approach is already used in geomorphological contexts allowing coarse-grained sediments and associated geomorphic processes that were hitherto not amenable to direct dating to be accurately temporally aligned (e.g. Jenkins et al. 2018; Rades et al. 2018; Bailiff et al. 2021; Cunningham et al. 2022).

Rock engravings

Luminescence rock surface exposure dating has the potential to be the first method that can be used to date the exposure of a freshly created archaeological or geological rock surface to sunlight. The timescale on which the method can work would be dictated by site-specific contexts, including the transparency/opacity of the lithology, rock-surface erosion rates, rates of weathering rind or varnish development, the dose rate of the rock, and the local insolation characteristics. However, if successfully applied, the method would allow the dating of any range of archaeological rock surfaces, including buildings, megaliths, and negative flake scars at palaeolithic quarries.

One exciting possibility is the use of luminescence rock surface exposure dating to directly date the timing of rock engravings, another site type that is currently undatable with currently available methods. An Australian Research Council-funded Linkage Project, ‘Dating Murujuga’s Dreaming’, is currently testing whether luminescence rock surface exposure dating can be applied to the globally significant rock engravings at Murujuga, Western Australia. The project also aims to use luminescence rock surface burial dating to date other stone features in the landscape, such as landscape walls, stone arrangements, and house structures. There are an estimated 1 million motifs across the archipelago, which are engraved into the weathering rind of Archean gabbro, granophyres, basalts, and fine-grained volcanoclastic sedimentary (FGS) rocks. Mulvaney (2015) developed a robust relative chronology for the region’s rock engravings based on the relationship between re-weathering of engraved surfaces (contrast state), superimposition of various motifs, the stylistic attributes of motifs, and the subject matter of motifs. The latter feature leverages the fact that Murujuga has been an archipelago since the early Holocene, before which it was > 100 km from the coast. Mulvaney (2015) identified seven major style phases, which he argues commence with the first settlement of the region—now known

to be 50,000 years ago (Veth et al. 2017) and continuing until AD 1842, where Aboriginal motifs are superimposed over dated whaler's inscriptions (Mulvaney et al. 2022). The aim of this project is to date various diagnostic motifs and provide absolute ages to anchor Mulvaney's (2015) relative chronology.

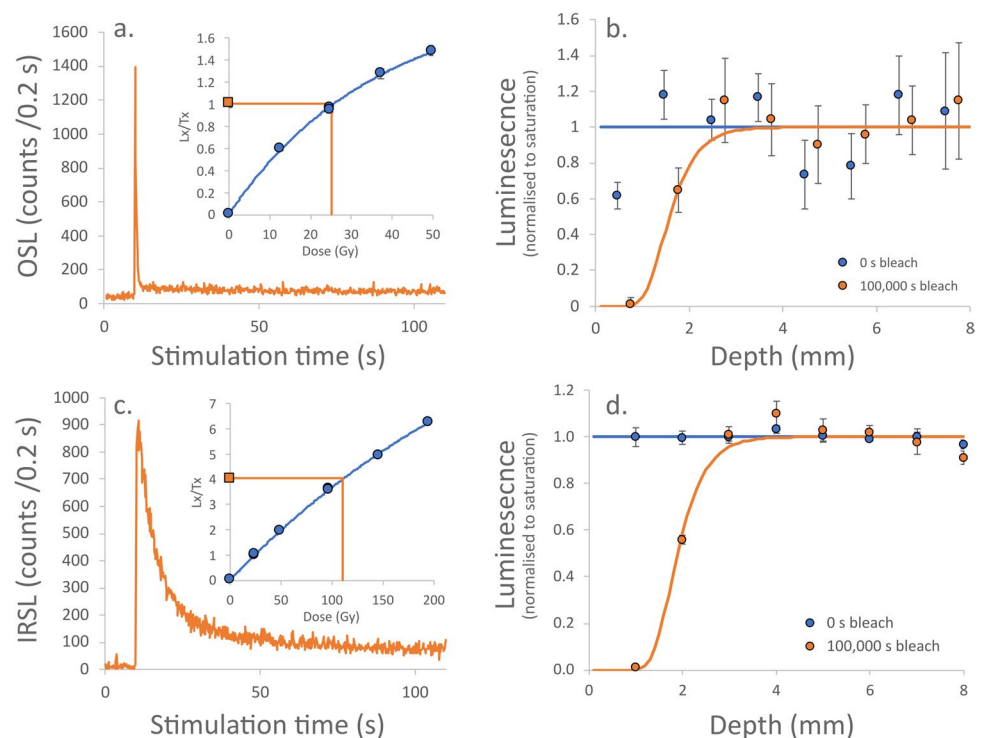
Given the igneous and meta-igneous lithologies that comprise Murujuga, the presence of usable and stable luminescence signals will be challenging. Polymineral aliquots of gabbro and granophyre yielded OSL (Fig. 13a) and IRSL (Fig. 13c) signals, respectively. Both signals were relatively dim, with the gabbro yielding ~1400 OSL counts and the granophyre yielding ~900 IRSL counts in the first channel. The gabbro OSL appears to be dominated by a fast-decaying OSL component. The corresponding dose response curves from dose recovery experiments (using 2×100 s blue LED bleaches) are shown in the inset of Fig. 13 a and c. The gabbro OSL signal could be used to recovery a given dose, with a measured/given dose ratio of 1.02 ± 0.02 ($n = 12$ aliquots). The granophyre IRSL signal yielded a residual-corrected measured/given dose ratio of 1.13 ± 0.05 ($n = 5$ aliquots). Next steps include completing a laboratory bleaching experiment following Gliganic et al. (2019). Cut rock surfaces from within a gabbro and granophyre boulder were cut into blocks, exposed to the solar simulator for durations ranging from 0 to 100,000 s, drilled, sliced, and measured. Preliminary luminescence-depth profiles shown in Fig. 13b and d show a mixed result. Promisingly, in both cases, the 100,000-s bleached block is bleached to a depth of 2 mm,

indicating that the luminescence signal in the rocks can be bleached and that the bleaching front can extend into the rock surface. Additionally, the 0-s bleached granophyre block is completely saturated up to the surface and there is generally little scatter in the Ln/Tn data. By contrast, the variability in the gabbro OSL-depth profiles, including the surface slice of the unbleached block, indicates that further signal characterisation work is required. Additionally, after the 100,000-s bleach, the inflection point of both gabbro and granophyre luminescence-depth profiles (50% saturation) is located at approximately 2 mm, which is relatively shallow; consider that after 100,000-s bleach, a quartzite was bleached to a depth of ~7 mm (Fig. 4a). This suggests that resolving luminescence-depth profiles in more opaque lithologies may be difficult with the current 1-mm-increment slicing approach and will require refined slicing procedures or spatially resolved 2D luminescence dating approaches (Sellwood et al. 2019, 2022; see below).

Chert

The examples and case studies of rock surface dating in archaeological contexts discussed so far were all conducted on macro-crystalline rocks including granites and granodiorites (Sohbati et al. 2015; Freiesleben et al. 2015; Feathers et al. 2022), metamorphic rocks such as paragneisses (Meyer et al. 2018; Ageby et al. 2021), or metamorphic quartz sandstone (i.e. quartzite, Gliganic et al. 2021) as well as unmetamorphic sedimentary rocks (Chapot et al. 2012; al Khasawneh et al.

Fig. 13 **a** Representative OSL decay curve from a polymineral aliquot of crushed gabbro from Murujuga, Western Australia following a 25 Gy beta dose. Inset shows the dose response curve built from the same aliquot as in **a**. **b** OSL-depth profiles from a laboratory bleaching experiment following Gliganic et al. (2019). The blue data are from an unbleached block and the orange data are from a block that was bleached for 100,000 s in a solar simulator. Note the bleached first slice of the bleached block's OSL-depth profile. **c** Representative IR50 decay curve from a polymineral aliquot of crushed granophyre from Murujuga, Western Australia following a 25 Gy beta dose. Inset shows a dose response curve. **d** IRSL-depth profiles shown as in **b**



2019a; al Khasawneh et al. 2019b). So far, attempts to also date micro- or crypto-crystalline materials such as chert or some volcanic rock types (e.g. andesites, basalts or dacites) via a rock surface dating approach are rare and produced results that were only partly consistent with independent age control (Morgenstein et al 2003; Feathers et al. 2019). Chert (in archaeological contexts sometimes also referred to as flint) is a chemically precipitated sedimentary rock composed primarily of silica usually with little contributions from other minerals (<5 to 25%; Blatt et al. 2006). Because of the excellent flaking properties of such micro- to crypto-crystalline materials, lithic tools are frequently made of chert or micro-crystalline volcanic rocks. However, the luminescence as well as the bleaching properties of these rock types have not been systematically investigated yet. To unleash the full potential of rock surface dating in archaeology (e.g. to directly date lithic artefacts from buried contexts or surface scatter sites, as described above), progress is required at this frontier.

Preliminary investigations into the luminescence and bleaching-with-depth properties of chert have been conducted using 26 chert artefacts from the wider realm of the European Alps ($n=20$), from Kazakhstan ($n=4$) and the Rocky Mountains (USA; $n=2$) (Meyer, in preparation). Small sub-samples from each chert artefact were investigated for the following properties using a Risø TL/OSL DA-20 reader: (i) the OSL signal (using a post-IR blue OSL approach; Banerjee et al. 2001) as part of a dose recovery test, (ii) the pIRIR225 signal (including the integrated IR50 signal) as part of a dose recovery test, and (iii) the resetting of the OSL and IR50 signals with depth into the artefacts in response to prolonged light exposure under a solar simulator (Hönle SOL 500). For the dose recovery tests, the sub-samples were crushed and the resulting chert flakes sieved to < 250 μm , mounted on stainless steel cups, and placed under the solar simulator to completely remove any remanent natural luminescence signal. Next a 30-Gy beta dose was administered and the aliquots were measured using the SAR protocol. Out of the 27 chert samples, 16 yielded dim but measurable OSL and/or IR50 signals. From 6 samples, a pIRIR225 signal could be measured too. Only 7 chert samples were big enough to also extract drill cores (9.7 mm diameter) in order to investigate the bleaching-with-depth properties of the OSL and IR50 signals. These 7 samples were first administered a 1-kGy gamma dose to ensure complete saturation before a single artefact surface of each sample was bleached via the Hönle SOL 500 for 48 h.

Figure 14 shows the results of three selected samples: JP10 (Fig. 14a), IR1 (Fig. 14b), and BP2 (Fig. 14c). The sensitivities of the OSL signals range from a few tens to several hundreds of counts in the initial channel of the OSL decay curves (Fig. 14d, e, f) and suitable dose response curves could be constructed for each of the samples Fig. 14g, h, i). The dose recovery ratios for samples IR1 and BP2

(0.98 ± 0.9 and 0.93 ± 0.07) were satisfactory, but sample JP10 (0.63 ± 0.10) underestimated the given dose. For two of these samples (IR1 and BP2), IR50 and pIRIR225 signals could be measured and dose response curves constructed (not shown). The OSL-depth profiles for all three samples are given in Fig. 14 j, k, and l and reveal that after 48 h the inflection point of the OSL-depth curve lies at $\sim 4\text{--}5\text{-mm}$ depth in the samples JP10 and BP2, and at $\sim 1\text{ mm}$ in sample IR1. It is concluded that (i) $\sim 50\%$ of the chert samples investigated in this preliminary study showed OSL and in some cases also IR and pIRIR luminescence signals; (ii) bleaching of even relatively dark chert types (e.g. sample IR1, Fig. 14b) is feasible, albeit at relatively slow bleaching rates; and (iii) further testing is required and should include investigations into signal stabilities, petrographic origin and fading properties of IRSL signals.

Developing measurement approaches

Finally, a new approach for measuring the luminescence signal from K-feldspar rich rocks was described by Sellwood et al. (2019, 2022) that may lead to a step change in the resolution at which measurements for rock surface dating can be undertaken. They circumvent the high labour cost, unwanted loss of material during coring and slicing, and low millimetre-scale resolution by directly 2D imaging the luminescence signal from rock slabs at a $\sim 140\text{-}\mu\text{m}$ scale using an EM-CCD camera. Such an imaging approach requires cutting the sample via a rock saw under controlled laboratory lighting conditions perpendicular to the rock surface of interest and imaging the cut plane using the camera system and appropriate stimulation sources. These spatially resolved luminescence measurements can reveal hundred-micrometre-resolved luminescence-depth profiles across several-centimetre-scale rock slabs (Sellwood et al. 2019, 2022). This enables the researcher to identify and overcome issues involving lithological heterogeneity in light attenuation (i.e. banding or patch shadowing), lithological heterogeneity in luminescent mineral phases, and light piping. Additionally, the higher resolution of luminescence measurements would increase the accuracy and precision of the 'depth' variable in luminescence-depth profiles, as well as enable the measurement of darker rocks with more compressed luminescence-depth profiles due to higher light attenuation. One complication is that EM-CCD cameras are considerably less sensitive than photo-multiplier tubes, thus requiring luminescence signals that are considerably brighter than is typically observed, which poses a problem for OSL and IRSL measurement. Sellwood et al. (2019) circumvent this issue by measuring the non-destructive IRPL (infrared photoluminescence) signal derived from K-feldspar in rocks. The same electron-trap pair can be resampled nearly infinitely, thereby enabling bright high-resolution IRPL (HR-IRPL) imaging and the construction of luminescence-depth

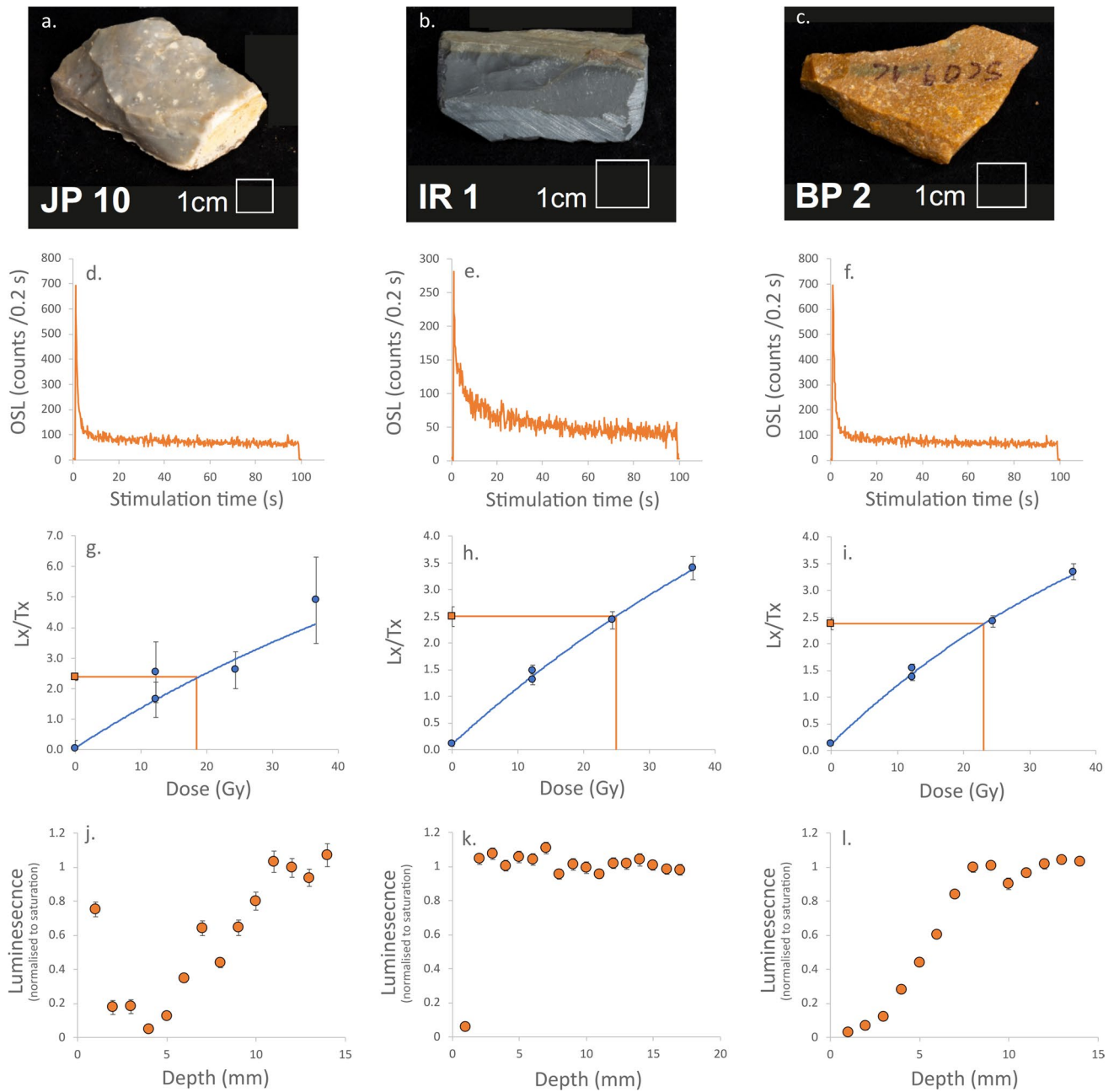


Fig. 14 Photographs, OSL decay curves, dose response curves, and OSL-depth profiles for three selected chert samples (European Alps, JP 10 (a); Kazakhstan, IR 1 (b); Rocky Mountains, BP 2 (c)) after administering a 30 Gy beta dose. The OSL decay curves were meas-

ured for 100 s stimulation with blue LEDs (d, e, f) and SAR dose response curves constructed (g, h, i). OSL-depth profiles are shown (j, k, l)

profiles with acceptable counting statistics. This approach is predicated on the rock type yielding a sufficiently bright and stable IRPL signal though. Given the novelty of this approach, archaeological dating applications using a CCD or EM-CCD setup are yet pending.

Conclusion

Luminescence rock surface dating approaches have enormous potential to contribute to the archaeological sciences. Studies have already used these approaches to constrain the

age of lithic artefact discard and post-depositional movement at surface scatter sites, to chronologically constrain rock art production by dating rockfall and exposure events, as well as dating a variety of rock-based archaeological features such as pavements, petroforms, megalithic structures, and walls. Current projects aim to use luminescence rock surface exposure dating to understand the age of Australian rock engravings and using luminescence rock surface burial dating to date megalithic features such as landscape walls and house structures, buried artefacts to circumvent complexity in sedimentary deposits, and more applications of surface artefact scatter dating. With ongoing work and applications, luminescence rock-surface dating has the potential to become widely applicable, shining new light on a diverse range of previously intractable archaeological contexts.

Author contribution L.A.G., J.M., and M.C.M. wrote the main manuscript text and L.A.G. prepared all figures. All authors reviewed the manuscript.

Funding This work was funded by an Australian Research Council grant to J.M. (LP190100724).

Declarations

Competing interests The authors declare no competing interests.

References

- Ageby L, Angelucci DE, Brill D, Carrer F, Rades EF, Rethemeyer J, Brückner H, Klasen N (2021) Rock surface IRSL dating of buried cobbles from an alpine dry-stone structure in Val di Sole, Italy. *Quaternary Geochronology* 66:101212. <https://doi.org/10.1016/j.quageo.2021.101212>
- Aitken MJ (1985) Thermoluminescence dating. Academic Press, London
- Aitken MJ (1998) An introduction to optical dating: the dating of Quaternary sediments by the use of photon-stimulated luminescence. Oxford University Press, Oxford
- Al Khasawneh S, Murray A, Abudana F (2019a) A first radiometric chronology for the Khatt Shebib megalithic structure in Jordan using the luminescence dating of rock surfaces. *Quaternary Geochronology* 49:205–210. <https://doi.org/10.1016/j.quageo.2018.02.007>
- Al Khasawneh S, Murray A, Thomsen K, AbuAzizeh W, Tarawneh M (2019b) Dating a near eastern desert hunting trap (kite) using rock surface luminescence dating. *Archaeological Anthropology Sci* 11(5):2109–2119. <https://doi.org/10.1007/s12520-018-0661-3>
- Alexanderson H (2022) Luminescence characteristics of Scandinavian quartz, their connection to bedrock provenance and influence on dating results. *Quat Geochronol* 69:101272
- Ames CJH, Gliganic L, Cordova CE, Boyd K, Jones BG, Maher L, Collins BR (2020) Chronostratigraphy, site formation, and palaeoenvironmental context of late Pleistocene and Holocene occupations at Grassridge Rock Shelter (Eastern Cape, South Africa). *Open Quaternary* 6(1):5. <https://doi.org/10.5334/oq.77>
- Auclair M, Lamothe M, Huot S (2003) Measurement of anomalous fading for feldspar IRSL using SAR. *Radiat Meas* 37:487–492
- Avner U, Shem-Tov M, Enmar L, Ragolski G, Shem-Tov R, Barzilai O (2014) A survey of Neolithic cult sites in the Eilat mountains, Israel. *Journal of Israel Prehistoric Society* 44:101–106
- Bailiff I, Bridgland D, Cunha PP (2021). Extending the range of optically stimulated luminescence dating using vein-quartz and quartzite sedimentary pebbles. *Quaternary Geochronology*, 101180
- Balek CL (2002) Buried artifacts in stable upland sites and the role of bioturbation: a review. *Geoarchaeol* 17(1):41–51
- Banerjee D, Murray AS, Botter-Jensen L, Lang A (2001) Equivalent dose estimation using a single aliquot of polymineral fine grains. *Radiat Meas* 33:73–94
- Blatt H, Tracy R, Owens B (2006) Petrology: igneous, sedimentary, and metamorphic, 3rd edn. W.H. Freeman & Company, New York
- Bowler JM, Johnston H, Olley JM, Prescott JR, Roberts RG, Shawcross W, Spooner NA (2003) New ages for human occupation and climatic change at Lake Mungo, Australia. *Nature* 421:20–23. <https://doi.org/10.1038/nature01391.1>
- Buylaert JP, Murray AS, Thomsen KJ, Jain M (2009) Testing the potential of an elevated temperature IRSL signal from K-feldspar. *Radiat Meas* 44:560–565
- Chapot MS, Sohbat R, Murray AS, Pederson JL, Rittenour TM (2012) Constraining the age of rock art by dating a rockfall event using sediment and rock-surface luminescence dating techniques. *Quat Geochronol* 13:18–25. <https://doi.org/10.1016/j.quageo.2012.08.005>
- Colarossi D, Duller GAT, Roberts HM, Tooth S, Lyons R (2015) Comparison of paired quartz OSL and feldspar post-IR IRSL dose distributions in poorly bleached fluvial sediments from South Africa. *Quat Geochronol* 30:233–238
- Cunningham A, Khashchevskaya D, Semikolennykh D, Kurbanov R, Murray A (2022) Luminescence dating of mass-transport sediment using rock-surface burial methods: a test case from the Baksan valley in the Caucasus Mountains. *Quat Geochronol* 68:101253
- Deviese, Thibaut, et al. Compound-specific radiocarbon dating and mitochondrial DNA analysis of the Pleistocene hominin from Salkhit Mongolia. *Nature Communications* 10.1 (2019): 274.
- Elkadi J, King GE, Lehmann B, Herman F (2021) Reducing variability in OSL rock surface dating profiles. *Quat Geochronol* 64:101169
- Feathers J, More GM, Quinterosc PS, Burkholder JE (2019) IRSL dating of rocks and sediments from desert geoglyphs in coastal Peru. *Quat Geochronol* 49:177–183. <https://doi.org/10.1016/j.quageo.2018.07.009>
- Feathers JK, Frouin M, Bench TG (2022) Luminescence dating of Enigmatic rock structures in New England, USA. *Quat Geochronol* 73:101402
- Fleming SJ (1966) Study of thermoluminescence of crystalline extracts from pottery. *Archaeometry* 9:170–173
- Freiesleben T, Sohbat R, Murray A, Jain M, al Khasawneh, S., Hvidt, S., & Jakobsen, B. (2015) Mathematical model quantifies multiple daylight exposure and burial events for rock surfaces using luminescence dating. *Radiat Meas* 81:16–22. <https://doi.org/10.1016/j.radmeas.2015.02.004>
- Freiesleben T, Thomsen KJ, Jain M (2022). Novel luminescence kinetic models for rock surface exposure dating. *Radiation Measurements*, 106877
- Fuhrmann S, Meyer MC, Gliganic LA, Obleitner F (2022) Testing the effects of aspect and total insolation on luminescence depth profiles for rock surface exposure dating. *Radiat Meas* 153:106732. <https://doi.org/10.1016/j.radmeas.2022.106732>

- Galli A, Martini M, Maspero F, Panzeri L, Sibilgia E (2014) Surface dating of bricks, an application of luminescence techniques. *The European Physical Journal plus* 129:101
- Galli A, Artesani A, Martini M, Sibilgia E, Panzeri L, Maspero F (2017) An empirical model of the sunlight bleaching efficiency of brick surfaces. *Radiat Meas* 107:67–72
- Galloway RB (2002) Does limestone show useful optically stimulated luminescence? *Ancient TL* 20(1):1–5
- Gliganic LA, Jacobs Z, Roberts RG, Domínguez-rodrigo M, Mabualla AZP (2012) New ages for Middle and Later Stone Age deposits at Mumba rockshelter, Tanzania : Optically stimulated luminescence dating of quartz and feldspar grains. *J Hum Evol* 62:533–547. <https://doi.org/10.1016/j.jhevol.2012.02.004>
- Gliganic LA, Cohen TJ, Slack M, Feathers JK (2016) Sediment mixing in aeolian sandsheets identified and quantified using single-grain optically stimulated luminescence. *Quat Geochronol* 32:53–66. <https://doi.org/10.1016/j.quageo.2015.12.006>
- Gliganic LA, Meyer MC, Sohbat R, Jain M, Barrett S (2019) OSL surface exposure dating of a lithic quarry in Tibet: laboratory validation and application. *Quat Geochronol* 49:199–204. <https://doi.org/10.1016/j.quageo.2018.04.012>
- Gliganic LA, Meyer MC, May J-H, Aldenderfer MS, Tropper P (2021). Direct dating of lithic surface artifacts using luminescence. *Science Advances*, 7(23)
- Godfrey-Smith DI, Huntley DJ, Chen W-H (1988) Optical dating studies of quartz and feldspar sediment extracts. *Quatern Sci Rev* 7:373–380
- Göksu HY, Fremlin JH, Irwin HT, Fryxell R (1974) Age determination of burned flint by a thermoluminescence method. *Science* 183:651–654
- Grün R (2006) Direct dating of human fossils. *Yearb Phys Anthropol* 49:2–48
- Habermann J, Schilles T, Kalchgruber R, Wagner GA (2000) Steps towards surface dating using luminescence. *Radiat Meas* 32(5–6):847–851. [https://doi.org/10.1016/S1350-4487\(00\)00066-4](https://doi.org/10.1016/S1350-4487(00)00066-4)
- Harris EC (1979) *Principles of archaeological stratigraphy*. Academic Press, London, New York
- Hellstrom J, Pickering R (2015) Recent advances and future prospects of the U-Th and U-Pb chronometers applicable to archaeology. *J Archaeol Sci* 56:32–40
- Huntley DJ, Baril MR (1997) The K content of the K-feldspars being measured in optical dating or in thermoluminescence dating. *Ancient TL* 15:11–13
- Huntley DJ, Hancock RGV (2001) The Rb contents of the K-feldspar grains being measured in optical dating. *Ancient TL* 19:43–46
- Huntley DJ, Lamothe M (2001) Ubiquity of anomalous fading in K-feldspars and the measurement and correction for it in optical dating. *Can J Earth Sci* 38:1093–1106
- Huntley DJ, Godfrey-Smith DI, Thewalt MLW (1985) Optical dating of sediments. *Nature* 313:105–107
- Hütt G, Jaek I, Tchonka J (1988) Optical dating: K-feldspars optical response stimulation spectra. *Quat Sci Rev* 7:381–385
- Jacobs Z, Roberts RG (2007) Advances in optically stimulated luminescence dating of individual grains of quartz from Archeological deposits. *Evolutionary Anthropology* 16:210–223
- Jacobs Z, Roberts RG, Galbraith RF, Deacon HJ, Grün R, Mackay A, Mitchell P, Vogelsang R, Wadley L (2008) Ages for the Middle Stone Age of Southern Africa: implications for human behavior and dispersal. *Science* 322(5902):733–735. <https://doi.org/10.1126/science.1162219>
- Jacobs Z, Meyer MC, Roberts RG, Aldeias V, Dibble H, el Hajraoui MA (2011) Single-grain OSL dating at La Grotte des Contrebandiers (‘Smugglers’ Cave’), Morocco: improved age constraints for the Middle Paleolithic levels. *J Archaeol Sci* 38(12):3631–3643. <https://doi.org/10.1016/j.jas.2011.08.033>
- Jenkins GTH, Duller GAT, Roberts HM, Chiverrell RC, Glasser NF (2018) A new approach for luminescence dating glaciofluvial deposits - high precision optical dating of cobbles. *Quatern Sci Rev* 192:263–273. <https://doi.org/10.1016/j.quascirev.2018.05.036>
- Jeong GY, Choi J-H (2012) Variations in quartz OSL components with lithology, weathering and transportation. *Quat Geochronol* 10:320–326
- Lehmann B, Herman F, Valla PG, King GE, Biswas RH (2019) Evaluating post-glacial bedrock erosion and surface exposure duration by coupling in situ optically stimulated luminescence and 10 Be dating. *Earth Surf Dyn* 7(3):633–662
- Leigh DS (1998) Evaluating Artifact burial by eolian versus bioturbation processes, South Carolina Sandhills, USA. *Geoarchaeology* 13(3):309–330
- Libby WF (1952) (1955), *Radiocarbon Dating*, 2nd edn. Chicago University Press, Chicago
- Liritzis I (1994) A new dating method by thermoluminescence of carved megalithic stone building. *Comptes Rendus de l’Académie des Sciences, Paris*, 319, serie II, 319: 603–610
- Liritzis I, Galloway RB (1999) Dating implications from solar bleaching of thermoluminescence of ancient marble. *J Radioanal Nucl Chem* 241(2):361–368. <https://doi.org/10.1007/BF02347476>
- Liritzis I, Vafiadou A (2015) Surface luminescence dating of some Egyptian monuments: case study. *J Cult Herit* 16:134–150
- Liritzis I, Drivaliari N, Polymeris GS, Katagas Ch (2010) New quartz technique for OSL dating of limestones. *Mediterr Archaeol Archaeom* 10:81–87
- Liritzis I, Polymeris GS, Vafiadou A, Sideris A, Levy TE (2019) Luminescence dating of stone wall, tomb and ceramics of Kastrouli (Phokis, Greece) Late Helladic settlement: Case study. *J Cult Herit* 35:76–85
- Lucas G (2012) *Understanding the archaeological record*. Cambridge University Press, New York
- McDonald J, Steelman KL, Veth P, Mackey J, Loewen J, Thurber CR, Guilderson TP (2014) Results from the first intensive dating program for pigment art in the Australian arid zone: insights into recent social complexity. *J Archaeol Sci* 46:195–204
- McDonald J, Reynen W, Petchey F, Ditchfield K, Byrne C, Vannieuwenhuyse D, Leopold M, Veth P (2018) Karnatukul (Serpent’s Glen): a new chronology for the oldest site in Australia’s Western Desert. *PLoS ONE* 13(9):e0202511
- McDougall I, Harrison TM (1999) *Geochronology and Thermochronology by the ⁴⁰Ar/³⁹Ar Method*. Oxford University Press, Oxford
- McDougall I, Brown FH, Fleagle JG (2005) Stratigraphic placement and age of modern humans from Kibish, Ethiopia. *Nature* 433:733–736
- McKeever S, Chen R (1997) Luminescence models. *Radiat Meas* 27(5–6):625–661
- Mejdahl, V. (1987). Internal radioactivity in quartz and feldspar grains. *Ancient TL*, 10–17
- Meyer MC, Gliganic LA, Jain M, Sohbat R, Schmidmair D (2018) Lithological controls on light penetration into rock surfaces – implications for OSL and IRSL surface exposure dating. *Radiat Meas* 120:298–304. <https://doi.org/10.1016/j.radmeas.2018.03.004>
- Meyer MC, Gliganic LA, May J-H, Merchel S, Rugel G, Schlütz F, Aldenderfer MS, Krainer K (2020) Landscape dynamics and human-environment interactions in the northern foothills of Cho Oyu and Mount Everest (southern Tibet) during the Late Pleistocene and Holocene. *Quatern Sci Rev* 229:106127. <https://doi.org/10.1016/j.quascirev.2019.106127>
- Moayed NK, Sohbat R, Murray AS, Rades EF, Fattahi M, Ruiz López JF (2023) Rock surface luminescence dating of

- prehistoric rock art from central Iberia. *Archaeometry* 65(2):319–334. <https://doi.org/10.1111/arc.12826>
- Morgenstein M, Luo S, Ku TL, Feathers J (2003) Uranium-series and luminescence dating of volcanic lithic artefacts. *Archaeometry* 45(3):503–518
- Mulvaney, K., E. Beckett and J. McDonald. (2022). *West Lewis Island rock art and stone structures*. In: Mulvaney, K. and J. McDonald (ed) *Murujuga: Dynamics of the Dreaming*. Rock art, stone features and excavations across the Dampier Archipelago. (CRAR+M Monograph No. 2). UWA Publishing, Perth
- Mulvaney, K. (2015) *Murujuga Marni*. Rock Art of the Macropod Hunters and Mollusc Harvesters. (CRAR+M Monograph; No. 1). UWA Publishing, Perth
- Murray AS, Wintle AG (2000) Luminescence dating of quartz using an improved single-aliquot regenerative-dose protocol. *Radiat Meas* 32:57–73
- Murray A, Arnold LJ, Buylaert J-P, Guérin G, Qin J, Singhvi AK, Smedley R, Thomsen KJ (2021) Optically stimulated luminescence dating using quartz. *Nature Rev Methods Primers* 1(1):1–31
- O’Gorman K, Tanner D, Sontag-González M, Li B, Brink F, Jones BG, Dosseto A, Jatmiko Roberts RG, Jacobs Z (2021) Composite grains from volcanic terranes: internal dose rates of supposed ‘potassium-rich’ feldspar grains used for optical dating at Liang Bua, Indonesia. *Quaternary Geochronology* 64:101182. <https://doi.org/10.1016/j.quageo.2021.101182>
- Ou XJ, Roberts HM, Duller GAT, Gunn MD, Perkins WT (2018) Attenuation of light in different rock types and implications for rock surface luminescence dating. *Radiat Meas* 120:305–311. <https://doi.org/10.1016/j.radmeas.2018.06.027>
- Peacock E, Fant DW (2002) Biomantle formation and artifact translocation in upland sandy soils: an example from the Holly springs national forest, North-Central Mississippi. *USA Geographical Archaeology* 17:91–114
- Pederson JL, Chapot MS, Simms SR, Sohbaty R, Rittenour TM, Murray AS, Cox G (2014) Age of Barrier Canyon-style rock art constrained by cross-cutting relations and luminescence dating techniques. *Proc Natl Acad Sci USA* 111(36):1–6. <https://doi.org/10.1073/pnas.1405402111>
- Polikreti K, Michael CT, Maniatis Y (2003) Thermoluminescence characteristics of marble and dating of freshly excavated marble objects. *Radiat Meas* 37(1):87–94. [https://doi.org/10.1016/S1350-4487\(02\)00088-4](https://doi.org/10.1016/S1350-4487(02)00088-4)
- Prasad AK, Poolton NRJ, Kook M, Jain M (2017) Optical dating in a new light: a direct, non-destructive probe of trapped electrons. *Sci Rep* 7:12097
- Prescott JR, Hutton JT (1994) Cosmic ray contributions to dose rates for luminescence and ESR dating: large depths and long-term time variations. *Radiat Meas* 23(1):497–500
- Rades EF, Sohbaty R, Lüthgens C, Jain M, Murray AS (2018) First luminescence-depth profiles from boulders from moraine deposits: insights into glaciation chronology and transport dynamics in Malta valley, Austria. *Radiat Meas* 120:281–289. <https://doi.org/10.1016/j.radmeas.2018.08.011>
- Rasheedy MS (1993) On the general-order kinetics of the thermoluminescence glow peak. *J Phys: Condens Matter* 5(5):633
- Richter D (2007) Advantages and limitations of thermoluminescence dating of heated flint from Paleolithic sites. *Geoarchaeology* 22(6):671–683
- Richter D, Krbetschek M (2006) A new thermoluminescence dating technique for heated flint. *Archaeometry* 48:695–705. <https://doi.org/10.1111/j.1475-4754.2006.00281.x>
- Rink WJ (1997) Electron spin resonance (ESR) dating and ESR applications in Quaternary science and archaeometry. *Radiat Meas* 27:975–1025
- Roberts RG, Lian OB (2015) Dating techniques: illuminating the past. *Nature* 520(7548):438–439
- Schaafsma P (1990) Shamans’ gallery: a Grand Canyon rock art site. *Kiva* 55(3):213–234
- Sellwood EL, Guralnik B, Kook M, Prasad AK, Sohbaty R, Hippe K, Wallinga J, Jain M (2019) Optical bleaching front in bedrock revealed by spatially-resolved infrared photoluminescence. *Sci Rep* 9(1):2611. <https://doi.org/10.1038/s41598-019-38815-0>
- Sellwood EL, Kook M, Jain M (2022) A 2D imaging system for mapping luminescence-depth profiles for rock surface dating. *Radiat Meas* 150:106697. <https://doi.org/10.1016/j.radmeas.2021.106697>
- Simms AR, DeWitt R, Kouremenos P, Drewry AM (2011) A new approach to reconstructing sea levels in Antarctica using optically stimulated luminescence of cobble surfaces. *Quat Geochronol* 6(1):50–60. <https://doi.org/10.1016/j.quageo.2010.06.004>
- Slack MJ, Law WB, Gliganic LA (2020) The early occupation of the Eastern Pilbara revisited: new radiometric chronologies and archaeological results from Newman Rockshelter and Newman Orebody XXIX. *Quatern Sci Rev* 236:106240. <https://doi.org/10.1016/j.quascirev.2020.106240>
- Smedley RK, Pearce NJG (2016) Internal U, Th and Rb concentrations of alkali-feldspar grains: implications for luminescence dating. *Quat Geochronol* 35:16–25. <https://doi.org/10.1016/j.quageo.2016.05.002>
- Sohbaty R, Murray AS, Jain M, Buylaert J-P, Thomsen KJ (2011) Investigating the resetting of OSL signals in rock surfaces. *Geochronometria* 38(3):249–258. <https://doi.org/10.2478/s13386-011-0029-2>
- Sohbaty R, Jain M, Murray A (2012a) Surface exposure dating of non-terrestrial bodies using optically stimulated luminescence: a new method. *Icarus* 221(1):160–166. <https://doi.org/10.1016/j.icarus.2012.07.017>
- Sohbaty R, Murray AS, Chapot MS, Jain M, Pederson J (2012b) Optically stimulated luminescence (OSL) as a chronometer for surface exposure dating. *J Geophys Res: Solid Earth* 117(9):1–7. <https://doi.org/10.1029/2012JB009383>
- Sohbaty R, Murray AS, Porat N, Jain M, Avner U (2015) Age of a prehistoric “Rodedian” cult site constrained by sediment and rock surface luminescence dating techniques. *Quat Geochronol* 30:90–99. <https://doi.org/10.1016/j.quageo.2015.09.002>
- Sohbaty R, Liu J, Jain M, Murray A, Egholm D, Paris R, Guralnik B (2018). Centennial- to millennial-scale hard rock erosion rates deduced from luminescence-depth profiles. *Earth and Planetary Science Letters*, 493, 218–230. <https://www.sciencedirect.com/science/article/pii/S0012821X18302127>
- Steelman KL et al (2021) Implications for rock art dating from the Lower Pecos Canyonlands, TX: A review. *Quat Geochronol* 63:101167
- Steelman, K. L. and M. W. Rowe 2012. Radiocarbon dating of rock paintings: incorporating pictographs into the archaeological record. In: J. McDonald and P. M. Veth (ed) *A Companion to Rock Art*. Wiley-Blackwell Publishing, Oxford
- Thomsen KJ, Murray AS, Jain M, Bøtter-Jensen L (2008) Laboratory fading rates of various luminescence signals from feldspar-rich sediment extracts. *Radiat Meas* 43(9–10):1474–1486. <https://doi.org/10.1016/j.radmeas.2008.06.002>
- van Calsteren P, Thomas L (2006) Uranium-series dating applications in Natural Environmental Science. *Earth Sci Rev* 75(1–4):155–175
- Veth P, Ward I, Manne T, Ulm S, Ditchfield K et al (2017) Early human occupation of a maritime desert, Barrow Island, North-West Australia. *Quatern Sci Rev* 168:19–29
- Vieilleigne E, Guibert P, Zuccarello AR, Bechtel F (2006) The potential of optically stimulated luminescence for medieval building: A case study at Termez, Uzbekistan. *Radiat Meas* 41:991–994

- Wilkins J, Schoville BJ, Pickering R, Gliganic L, Collins B, Brown KS, von der Meden J, Khumalo W, Meyer MC, Maape S, Blackwood AF, Hatton A (2021) Innovative *Homo sapiens* behaviours 105,000 years ago in a wetter Kalahari. *Nature* 592(7853):248–252. <https://doi.org/10.1038/s41586-021-03419-0>
- Wintle AG (1973) Anomalous fading of thermoluminescence in mineral samples. *Nature* 245:143–144
- Wintle AG (1997) Luminescence dating: laboratory procedures and protocols. *Radiat Meas* 27:769–817
- Wintle AG, Murray AS (2006) A review of quartz optically stimulated luminescence characteristics and their relevance in single-aliquot regeneration dating protocols. *Radiat Meas* 41(4):369–391. <https://doi.org/10.1016/j.radmeas.2005.11.001>
- Zimmerman DW (1967) Thermoluminescence from fine grains from ancient pottery. *Archaeometry* 10:26–28

Publisher's Note Springer Nature remains neutral with regard to jurisdictional claims in published maps and institutional affiliations.

Springer Nature or its licensor (e.g. a society or other partner) holds exclusive rights to this article under a publishing agreement with the author(s) or other rightsholder(s); author self-archiving of the accepted manuscript version of this article is solely governed by the terms of such publishing agreement and applicable law.